GJBX-59(78)

GROSS GAMMA-RAY CALIBRATION BLOCKS

Bendix Field Engineering Corporation
Grand Junction Operations
Grand Junction, Colorado 81501

May 1978

ISSUED BY THE U.S. DEPARTMENT OF ENERGY
GRAND JUNCTION OFFICE
UNDER CONTRACT NO. EY-76-C-13-1664

GJBX-59(78)

GROSS GAMMA-RAY CALIBRATION BLOCKS

PART I. GROSS GAMMA-RAY CALIBRATION BLOCKS; CONSTRUCTION

Mark A. Mathews

PART II. GROSS GAMMA-RAY CALIBRATION BLOCKS; GRADE ASSIGNMENT

Kenneth L. Kosanke

January 1976

Issued May 1978

Prepared for the U.S. Department of Energy
under Contract No. EY-76-C-13-1664, BFEC

GROSS GAMMA-RAY CALIBRATION BLOCKS

ABSTRACT

Eleven transportable, portable hand counter or face scanner calibration blocks were constructed from predetermined mixtures of sand, uranium ore, and concrete. Each block, a cylinder 42 inches in diameter and 17 inches deep, is a standard calibration source. These blocks approximate an infinite source, in both the vertical and horizontal directions, for the gamma-rays of interest.

The grades assigned to these blocks, for the purpose of calibrating portable gross gamma detectors, were determined by a procedure based on a standard least-squares technique for limiting sampling errors. Calibration to these grades is necessary to determine if the counters are properly functioning and to estimate uranium ore grades in the field.

The grades assigned to the blocks are:

Block Number		Assigned Dry Weight	
		Percent eU_3O_8	ppm eU
GJ	50	0.0094 ± 0.0003	80 ± 3
GJ	200	0.0303 ± 0.0006	257 ± 5
LASL	500	0.0720 ± 0.0011	611 ± 9
GJ	1000	0.144 ± 0.002	1220 ± 20
GJ	3000	0.334 ± 0.004	2830 ± 40
CW	200	0.0313 ± 0.0006	265 ± 5
CW	1000	0.149 ± 0.002	1260 ± 20
GWT	200	0.0316 ± 0.0006	268 ± 5
GWT	1000	0.147 ± 0.002	1250 ± 20
GNM	200	0.032 ± 0.0006	272 ± 5
GNM	1000	0.145 ± 0.002	1230 ± 20

Prefix Definitions:

GJ These blocks will remain at Grand Junction, Colorado.
LASL This block was sent to Los Alamos Scientific Laboratory.
CW These blocks were sent to Casper, Wyoming.
GNM These blocks were sent to Grants, New Mexico.
GWT These blocks were sent to George West, Texas.

SUMMARY OF CONTENTS

PART I. GROSS GAMMA-RAY CALIBRATION BLOCKS, CONSTRUCTION

ABSTRACT

Eleven transportable calibration blocks were constructed to calibrate portable hand counters (gross gamma) or face scanners. These blocks consist of sand, uranium ore, and concrete mixtures which were poured into containers 42 inches in diameter and 17-18 inches in depth. Each block is regarded as a standard calibration source that approximates as infinite thickness, in both vertical and horizontal directions, for the gamma-ray energies of interest. These blocks and their grade assignments provide calibration facilities which can be used by BFEC and DOE personnel as well as private industry. Calibration is necessary to determine if the counters or scanners are functioning properly and to estimate the uranium ore grade encountered in the field.

PART I

CONTENTS

TABLES

FIGURES

CONTENTS (cont'd.)

APPENDICES

CONTENTS (cont'd.)

PART II

CONTENTS

TABLES

FIGURES

CONTENTS (cont'd)

GROSS GAMMA-RAY (HAND COUNTER) CALIBRATION BLOCKS; CONSTRUCTION

Introduction

Portable hand counters (gross gamma) or face scanners are calibrated to determine if they are functioning properly and to estimate the grade of uranium ore encountered in field surveys. Standard calibration sources, approximating an infinite thickness in both vertical and horizontal directions for the gamma-ray energies of interest, are used to calibrate these counters. These standard calibration sources, called blocks, also simulate the geologic environment (rock, concentration range, etc.) where the gamma counters or face scanners are used.

Eleven portable calibration blocks were constructed to the above criterion. Each block consists of a sand, uranium ore, and concrete mixture poured into a container, 17-18 inches in depth, consisting of a 42-inch diameter, corrugated, galvanized culvert, which is open at the top and closed at the lower end with 3/16-inch sheet metal (approximately 1 meter in diameter by 1/2 meter in depth). The nominal design grades for these blocks ranged from 50 to 3000 ppm uranium (U) concentration. Four blocks were installed at the DOE Grand Junction Office with nominal design grades of 50, 200, 1000,and 3000 ppm uranium concentration. Two blocks were installed at each of the existing field logging model sites (Grants, New Mexico; George West, Texas; and Casper, Wyoming); their nominal design grades were 200 and 1000 ppm uranium concentration. One block, having a nominal design grade of 500 ppm uranium concentration, was installed at Los Alamos Scientific Laboratory (LASL).

The nominal design grade of each block differs from the actual grade assigned to each block because of the distribution uncertainties that occur during construction.*

---

*The grade assigned to each block and the methods used to obtain the grade are discussed in Part II of this report, "Gross Gamma-Ray Calibration Blocks: Grade Assignment".

Physical Construction

The serial numbers, 1 through 11, are used to describe the calibration blocks in this report (see Table I-I). The size of each block is about 1 meter in diameter and 1/2 meter in depth and approximates an infinite thickness, in both the vertical and horizontal directions, to the gamma rays of interest. Each block is enclosed in a metal container made from corrugated, galvanized culvert that is 42 inches in diameter and 17-18 inches deep. The culvert is closed at the lower end with 3/16-inch sheet metal and has a removable metal cover on the upper end. Plastic sheeting was used to line the bottom and sides of the container to protect these calibration sources from weathering (Fig. I-I).

Each block contains a mixture of sand, uranium ore, and cement. The uranium ore for each block was ground to a minus-10 mesh in an Englebach pulverizer and Table I-II lists the type (Schwartzwalder, Climax, Monument Valley) and grade of uranium ores used. A list of the types of materials and the quantities used in constructing these blocks is given in Table I-III. The ground uranium ore and plaster sand were blended for each design grade (50, 200, 500, 1000, and 3000 ppm U) and stored in barrels. A 5-pound sample of each design grade was taken from the barrels using a Jones splitter; this sample and a 5-pound sample of the plaster sand yield reasonably representative samples of the mixtures. These samples were analyzed by the Chemistry and Petrology Laboratories; the results are listed in Table I-IV.

The analytical assay values of the various sand and uranium ore mixtures, when computationally blended with the originally planned amounts of cement and water, produced calibration blocks that have grades slightly higher in ppm U than the original design grades. These grades, although slightly higher than planned, were considered sufficiently close to the design grades to proceed with the project of mixing the sand-uranium ore blend with cement and water. The blended

TABLE I-I

Identification of Calibration Blocks Constructed

Serial Number	Identification of the Block	Government ID Number
1	GJ 50	GJO 10253
2	GJ 200	GJO 10254
3	LASL 500	GJO 10257
4	GJ 1000	GJO 10255
5	GJ 3000	GJO 10256
6	CW 200	GJO 10130
7	CW 1000	GJO 10131
8	GNM 200	GJO 10132
9	GNM 1000	GJO 10133
10	GWT 200	GJO 10134
11	GWT 1000	GJO 10135

The letters in the identification of the block are the location of each block.

GJ - Grand Junction
LASL - Los Alamos Scientific Laboratory
CW - Casper, Wyoming
GNM - Grants, New Mexico
GWT - George West, Texas

The numbers in the identification block are the nominal uranium concentration design grades.

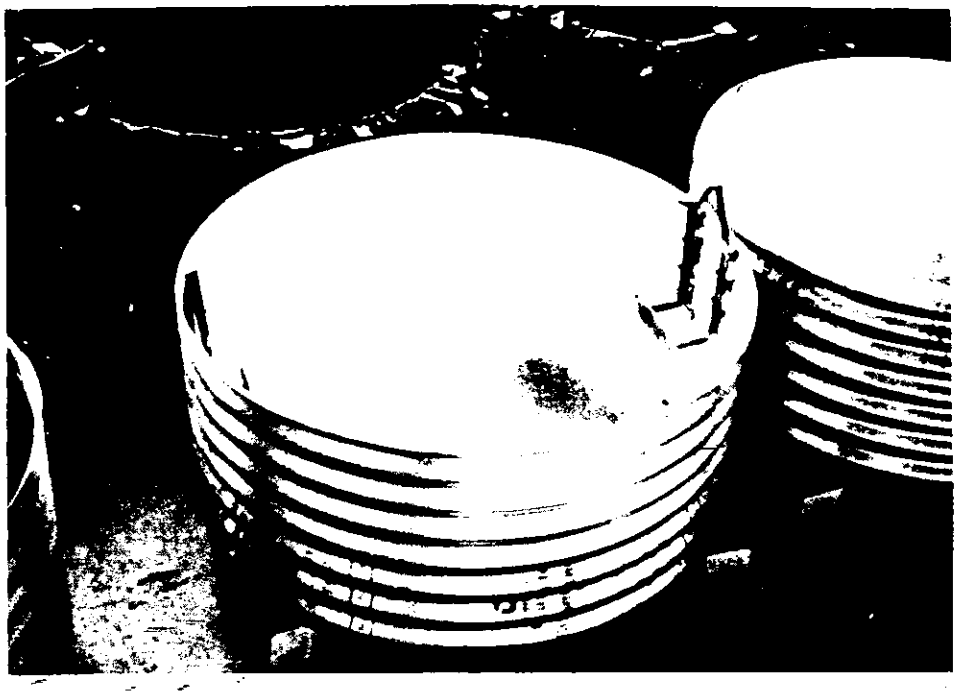

Figure I-I. Calibration Block Container

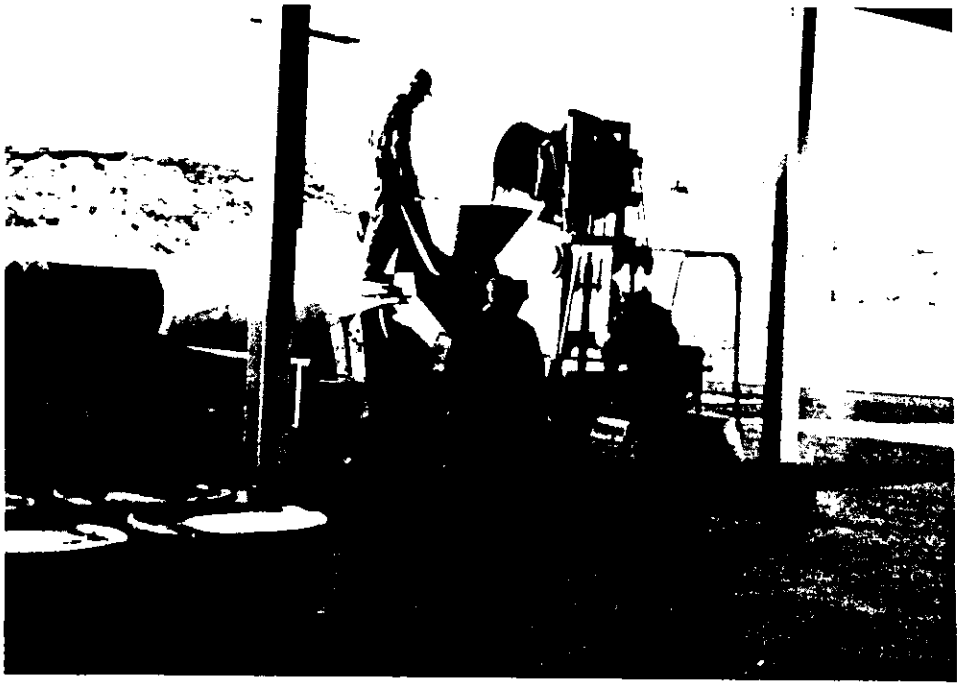

Figure I-II. Mixing Ingredients for Blocks

Ore Type Used for Calibration Blocks

Calibration Blocks Serial Numbers	Ore Type	Chemical Assay % U_3O_8	Radiometric Assay (Gross Gamma) % eU_3O_8
1 through 10	Residue from New Water Factor Model	0.326	0.315
11	Schwartzwalder	2.77	2.83

Ore Used for New Water Factor Model

Ore Type	Amount-lbs	Chem Assay % U_3O_8	Gross Gamma Assay % eU_3O_8
Climax	4632	0.134	0.301
Schwartzwalder	1553	2.924	3.008
Residue from U-2 test pit	1885	1.172	1.107
Residue from U-3 test pit	2260	0.426	0.418

Ore Used for U-1 Log Model

Ore Type	Amount-lbs	Gross Gamma Assay % eU_3O_8
Schwartzwalder	430.8	11.19
Schwartzwalder	4861.7	2.62

Ore Used for U-2 Log Model

Ore Type	Amount-lbs	Gross Gamma Assay % eU_3O_8
Schwartzwalder	1980	2.62
Residue from U-1 test pit	716	2.422
Residue Texas high grade pit	1413	2.205
Residue C test pit	1480	0.280

Ore Used for U-3 Log Model

Ore Type	Amount-lbs	Gross Gamma Assay % eU_3O_8
Schwartzwalder	1653	2.62
Schwartzwalder	689	0.287
Residue Texas low grade pit	1925	0.257
Residue C test pit	1821	0.280

Ore Used for C Log Model

Ore Type	Amount-lbs	Gross Gamma Assay % eU_3O_8
Schwartzwalder	17000	0.287
Monument Valley	240	4.64

Ore Used for Casper High Grade Log Model

Ore Type	Amount-lbs	Gross Gamma Assay % eU_3O_8
Schwartzwalder	4101	3.00
Schwartzwalder	336	0.254

Ore Used for Texas High Grade Log Model

Ore Type	Amount-lbs	Gross Gamma Assay % eU_3O_8
Schwartzwalder	3376	3.00
Schwartzwalder	100	0.254
Monument Valley	240	4.00
Residue Casper high grade pit	1461	2.187

Ore Used for Texas Low Grade Log Model

Ore Type	Amount-lbs	Gross Gamma Assay % eU_3O_8
Schwartzwalder	2298	0.254
Monument Valley	260	4.00
Residue Grants low grade pit	1796	0.306
Dry Texas sand	819	?

Ore Used for Grants Low Grade Log Model

Ore Type	Amount-lbs	Gross Gamma Assay % eU_3O_8
Schwartzwalder	4140	0.254
Schwartzwalder	297	3.00

sand and uranium ore for each design grade was put into the hopper of a cement mixing truck and mixed as the truck returned to the bulk plant for cement and water (Figure I-II). Table I-III lists the materials used for the 5 design grades and 11 calibration blocks. The sand, uranium ore, cement, and water of each design grade were thoroughly mixed (20-30 minutes) as the cement truck returned to the GJO compound. The batch was then poured into the containers (Fig. I-III).

Sample Acquisition and Analysis

The following samples were collected during each of the calibration block pours: three 1-quart cardboard ice cream cartons were obtained at the bottom, middle, and top of the block; and one metal can (for gamma-ray spectroscopy) was obtained at the middle of the block (Fig. I-IV and I-V). Each gamma-ray spectroscopy (gamma-spec) can sample was weighed at the time it was collected and allowed to cure for 30 days and again weighed. This procedure yields an estimate of the moisture content of the calibration block. Laboratory analyses (chemical and radiometric) were performed on these samples and these results are listed in Table I-V.

The surfaces of the blocks were finished smooth (Fig. I-VI) and the blocks were allowed to set for 35 days in a heated garage. Then the blocks were cored (Fig. I-VII and I-VIII) and these cores (2 1/2-inch diameter) were analyzed for moisture content and density. The moisture content of the cores were compared to the calculated moisture content from the gamma-spec can samples. These results are listed in Table I-VI.

The semi-quantitative spectrographic analysis (element comparison percent) of the materials used in the construction of the calibration blocks is listed in Appendix A-I. The petrographic analyses (mineralogy identification) of the materials used in the construction of the calibration blocks are listed in Appendix B-I.

TABLE I-III

Materials Used in Calibration Blocks

Calibration Block Serial Number (Design Grade)	Uranium Ore lbs	Sand lbs	Cement lbs	Water gallons - lbs
4, 7, 9, 11 (1000)	2380	2892	1680	160-1336
2, 6, 8, 10 (200)	475	4841.7	1680	140-1169
5 (3000)	194	1124.6	420	27-225.5
3 (500)	296	1019.3	420	37-309
1 (50)	30	1296.1	420	37-309

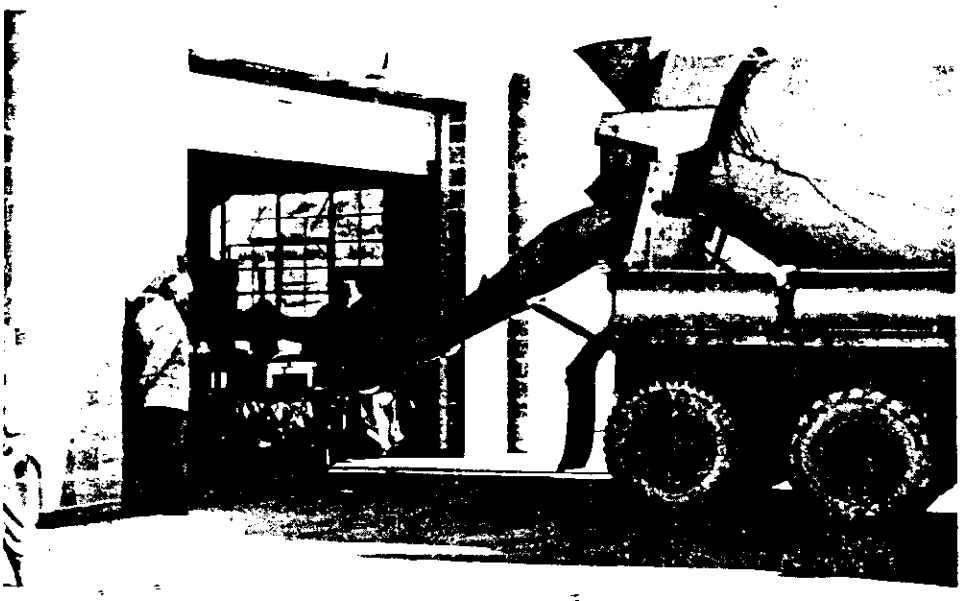

Figure I-III. Pouring Batch in Calibration Block Containers

Figure I-IV. Metal Can Gamma-spec Sample

Figure I-V. Quart Cardboard Ice Cream Carton Samples

Figure I-VI. Finishing Surface of Calibration Block

TABLE I-IV

Laboratory Analyses of Mixtures

Sample Number	Representative Material	Chem Analysis* % U_3O_8	Gamma Only Analysis* % eU_3O_8 - sample wt.	Spectral Scintillation*				Spectral Ge(Li)*				Emission Spectrographic Analysis*	Petrographic Analysis*
				%	ppm		sample	%	ppm		sample		
				K	Th	U	weight	K	ThO_2	U_3O_8	weight		
16604	plaster sand	0.004	0.001 - 23.381 g	1.80	8.4	2.1	739.320 g					See Appendix A	See Appendix B
16605	200 ppm U blocks	0.042	0.038 - 20.262 g	1.54	18.6	277.5	747.810 g					See Appendix A	See Appendix B
16606	1000 ppm U blocks	0.190	0.186 - 21.551 g					2.04±0.49	0	1694±24	712.20 g	See Appendix A	See Appendix B
16833	50 ppm U block	0.011 or 93 ppm U		1.82	9.5	66.2	722.010 g					See Appendix A	See Appendix B
16834	500 ppm U block	0.104	0.100 - 24.474	1.56	27.5	698.5	714.610 g					See Appendix A	See Appendix B
17064	3000 ppm U block	0.412	0.426 - 21.756					0	0	3874±39	728.21 g	See Appendix A	See Appendix B

* Dry weight basis.

TABLE I-V

Laboratory Analyses of Block Samples

Calibration Block Serial Number	Sample Number	Chem Assay % U_3O_8	Gross Gamma % eU_3O_8	Radiometric Analyses: Spectral Scintillation %	Spectral Scintillation ppm Th	Spectral Scintillation ppm U	Spectral Ge(Li) %	Spectral Ge(Li) ppm Th	Spectral Ge(Li) ppm U	Relative Emanation Coefficient	Density g/cc	
1 B	17406	0.007	0.0071(d)	1.60	5.7	62.8				(a)	1.90	
1 M	17407	0.007	0.0077(d)	1.74	7.0	67.2				(a)	1.88	
1 M	17748			1.40	7.9	62.1	1.31	1.1	58.4	(c)		
1 T	17408	0.008	0.0079(d)	1.54	5.6	70.2				(a)	1.89	
2 B	17409	0.028	0.038	1.46	14.7	235				0.34	1.83	
2 M	17410	0.027	0.030	1.62	15.2	240				0.15	1.84	
2 M	17749			1.44	21.2	201.3	1.22	1.4	197.5	(c)		
2 T	17411	0.028	0.038	1.39	16.1	242				0.30	1.85	
3 B	17412	0.079	0.083	1.94	21	563				0.16	1.87	
3 M	17413	0.072	0.078	1.36	22.6	560				0.22	1.88	
3 M	17750			1.39	19.6	473.2	1.12	1.8	472.4	(c)		
3 T	17414	0.060	0.067	1.48	23.7	557				0.20	1.87	
4 B	17415	0.134	0.146	2.47	41.6	1164				0.20	1.85	
4 M	17416	0.137	0.144	2.63	40.9	1138				0.18	1.84	
4 M	17751			1.58	36.6	968	0.26	1.1	934.7	(c)		
4 T	17417	0.141	0.146	2.30	38.8	1138				0.18	1.84	
5 B	17418	0.295	0.326	1.51	87.9	2440.4				0.13	1.94	
5 M	17419	0.295	0.334	10.12	99.3	2399				0.20	1.95	
5 M	17752			3.46	79.6	2141.2	1.10	1.2	954.2	(c)		
5 T	17420	0.308	0.330	1.76	94.2	2405.5				0.14	1.94	
6 B	17433	0.032	0.033	1.40	12.5	240				0.32	1.83	
6 M	17434	0.032	0.033	1.35	14.0	235				0.20	1.82	
6 M	17757			1.41	11.6	192.2	1.22	3.9	184.1	(c)		
6 T	17435	0.033	0.035	14.8	1.56	226.9				0.23	1.84	
7 B	17436	0.151	0.152	1.79	39.1	1194				0.16	1.86	
7 M	17437	0.145	0.160	1.24	43.4	1134				0.22	1.85	
7 M	17758			1.27	33.5	958	1.29	1.9	932.1	(c)		
7 T	17438	0.141	0.147	1.08	41.9	1141.5				0.20	1.86	
8 B	17427	0.033	0.030	1.60	12.1	242				(b)	1.88	
8 M	17428	0.031	0.030	1.67	11.9	237				0.26	1.84	
8 M	17755			1.45	12.7	209.3	1.29	1.5	207.8	(c)		
8 T	17429	0.033	0.029	1.48	14.9	232.4				0.13	1.84	
9 B	17430	0.142	0.150	0.91	42.9	1102.9				0.19	1.84	
9 M	17431	0.142	0.145	0.93	43.3	1112.7				0.17	1.84	
9 M	17756			1.52	34.7	943.4	1.24	3.8	977.9	(c)		
9 T	17432	0.141	0.146	0.92	45.6	1189.6				0.17	1.83	
10 B	17421	0.031	0.037	1.36	12.3	238				0.34	1.83	
10 M	17422	0.032	0.032	1.46	14.2	236				0.21	1.86	
10 M	17753			1.27	12	197.4	1.30	1.1	189	(c)		
10 T	17423	0.030	0.029	1.52	15	231.2				0.04	1.86	
11 B	17424	0.133	0.136	0.81	43.7	1185.8				0.15	1.85	
11 M	17425	0.133	0.143	2.04	37.9	1172				0.15	1.86	
11 M	17754			1.45	37.2	985.6	1.10	2.5	956.7	(c)		
11 T	17426	0.138	0.152	2.14	38.5	1119				0.16	1.83	
Cement Sample	17439	0.0004		0.50	5.6	3.1				(c)	1.86	

(a) The original samples from this block were contaminated in the sampling plant and had to be reprepared from remaining sample material. No relative emanation coefficient was obtained.

(b) No emanation coefficient was calculated because second count rate was lower than first.

(c) No emanation coefficient was calculated.

(d) Extended data collection times were used for this sample to improve the statistical precision of the data.

Figure I-VII. Coring Calibration Block

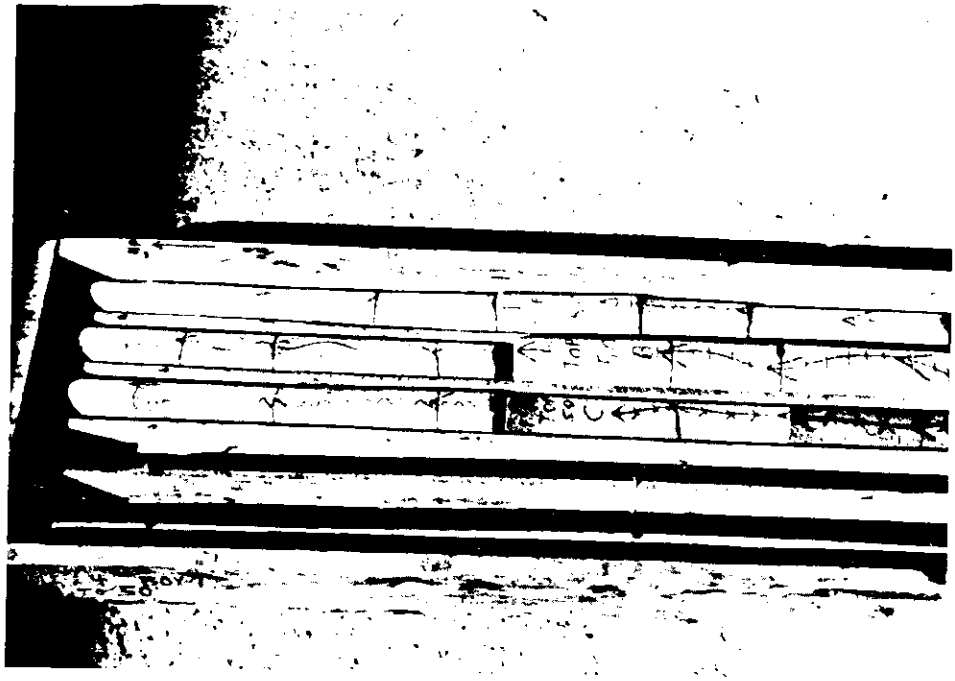

Figure I-VIII. Calibration Block Cores

TABLE I-VI

Density and Moisture Analyses

Calibration Block Serial Number	Core Sample			Gamma-Spec Can With Sample			
	number	density g/cc	±LOD	number	at time sample taken	30 days later	Moisture from and hydrated
1 Core A	17848	1.86	2.64	17748	829.00	762.70	7.65
	17849	1.86	2.84				
	17850	1.87	2.75				
	17851	1.87	2.45				
	average	1.87	2.67				
Core B	17856	1.87	2.79				
	17857	1.85	3.02				
	17858	1.86	2.70				
	17859	1.87	2.24				
	17860	1.85	2.77				
	average	1.86	2.70				
Core C	17861	1.87	3.03				
	17862	1.86	2.72				
	17863	1.88	2.23				
	average	1.87	2.66				
2	17852	1.84	2.71	17749	804.32	748.12	7.78
	17853	1.83	3.19				
	17854	1.82	Lost				
	17855	1.83	2.49				
	average	1.83	2.80				
3	17867	1.85	2.74	17750	811.52	753.32	8.56
	17868	1.85	3.07				
	17869	1.85	3.09				
	17870	1.87	2.82				
	average	1.86	2.93				
4	17871	1.82	3.64	17751	850.74	780.34	8.55
	17872	1.83	3.57				
	average	1.83	3.61				
5 Core A	17864	1.91	2.53	17752	870.39	798.39	3.50
	17865	1.92	2.88				
	17866	1.93	2.81				
	average	1.92	2.74				
Core B	17873	1.92	2.63				
	17874	1.91	2.93				
	17875	1.92	3.21				
	17876	1.93	2.87				
	average	1.92	2.91				
Core C	17877	1.94	2.46				
	17878	1.92	2.82				
	17879	1.93	3.03				
	17880	1.94	2.85				
	average	1.93	2.79				
6	17896	1.85	2.38	17757	844.21	787.71	8.17
	17897	1.83	2.71				
	17898	1.82	2.87				
	17899	1.84	2.77				
	average	1.84	2.68				
7	17900	1.83	3.62	17758	835.38	767.38	8.69
	17901	1.83	3.52				
	average	1.83	3.57				
8	17889	1.85	2.41	17755	807.58	751.58	7.94
	17890	1.83	2.44				
	17891	1.85	2.36				
	17892	1.84	2.54				
	17893	1.83	2.40				
	average	1.84	2.43				
9	17894	1.83	3.54	17756	842.80	773.30	8.32
	17895	1.83	3.58				
	average	1.83	3.56				
10	17881	1.86	2.43	17753	857.43	800.43	8.22
	17882	1.85	2.52				
	17883	1.83	2.57				
	17884	1.84	2.40				
	17885	1.86	2.41				
	17886	1.88	2.38				
	average	1.85	2.45				
11	17887	1.83	3.56	17754	820.91	751.81	8.41
	17888	1.83	3.59				
	average	1.83	3.58				

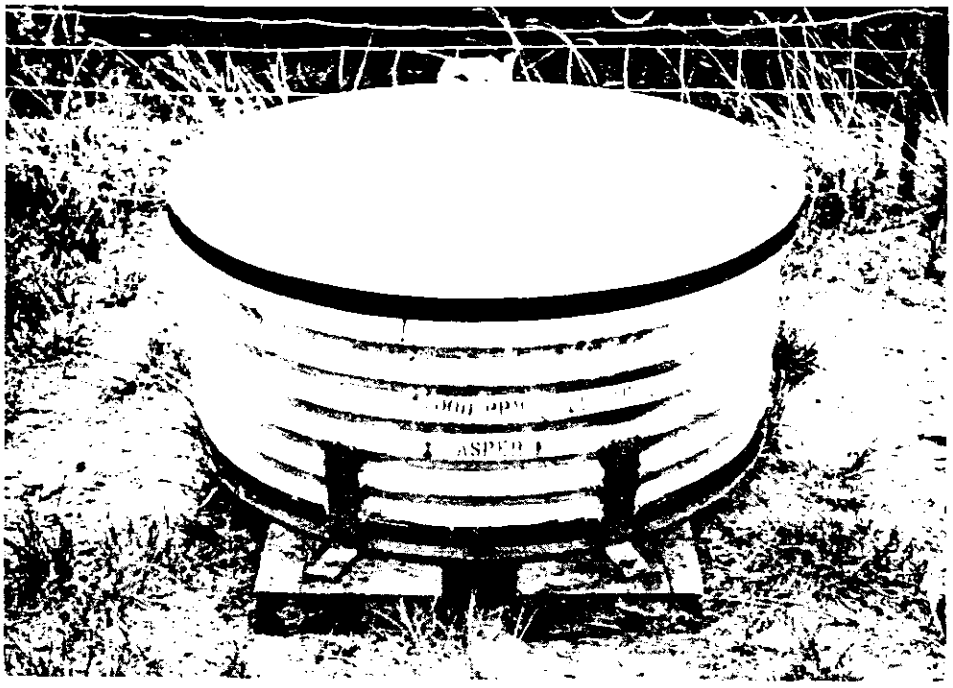

Figure I-IX. Completed Calibration Block

Figure I-X. Calibration Blocks at Casper, Wyoming Field Calibration Site

Conclusions

Construction of the blocks was completed by mounting the blocks on wooden planks, cutting the edge of the container so that they were flush with the concrete, and fabricating easily removed lids to protect the block from the weather (Fig. I-1X). A brass plug that identifies the block and its grade (ppm U) was set in the surface of each block. Figure I-X shows the location of the two gross gamma calibration blocks at a field calibration site (Casper, Wyoming). The block location and positioning are similar at the other field calibration sites.

These blocks and the data obtained from sample analyses from the blocks provide calibration facilities for portable, gross gamma counters or face scanners, which can be used by DOE-BFEC personnel and private industry to determine whether or not counters or scanners are functioning properly and to estimate the grade of uranium ore encountered by scanners in the field*.

*More details concerning DoE calibration facilities appear in "A Review of U.S. DoE Calibration Facilities" by Hilton B. Evans, February, 1978.

APPENDIX AI

EMISSION SPECTROGRAPHIC ANALYSES OF TEST BLOCK MATERIAL

REQUISITION NUMBER 400006
DATE 11/03/75

SEMIQUANTITATIVE EMISSION SPECTROGRAPHIC ANALYSIS
ELEMENT COMPARISON IN PERCENT

LPI NO.	16604	16605	16606
AG	0	0	.0010
AL	8.0000	9.0000	10.0000
AS	0	0	.0500
B	.0030	.0040	.0070
BA	.1500	.1500	.1000
BE	.0003	.0005	.0007
BI	0	0	.0010
CA	3.0000	4.0000	9.0000
CD	.0010	.0020	.0020
CR	.0020	.0030	.0060
CU	.0050	.0040	.0100
FE	2.5000	2.0000	1.5000
GA	.0001	.0001	.0003
K	1.5000	1.5000	2.5000
LI	.0010	.0020	.0100
MG	.3000	.3000	.6000
MN	.0500	.0600	.0700
MO	0	.0080	.0200
NA	1.5000	1.5000	2.5000
NI	.0010	.0030	.0070
P	.0200	.0100	.0100
PB	.0008	.0010	.1300
RB	0	0	.0100
SB	0	0	.0020
SI	10.9999	10.9999	10.9999
SN	0	0	.0005
SR	.0600	.0700	.1500
TI	.1500	.1500	.1000
V	.0040	.0200	.2000
Y	.0020	.0020	.0010
ZN	.0100	.0200	.0700
ZR	.0100	.0100	.0200

ELEMENTS NOT FOUND:
AU CD CE CS DY ER EU GD GE HF HG HO IN IR LA LU NB ND OS PD PR PT RE RH RU SC SE SM TA TB TE TH TL TM U W YB

X.9999 DESIGNATES A CONCENTRATION GREATER THAN X PERCENT.

I FIND 0060 STOP
EOJ

REQUISITION NUMBER 40000H
DATE 01/16/76

SEMIQUANTITATIVE EMISSION SPECTROGRAPHIC ANALYSIS
ELEMENT COMPARISON IN PERCENT

LPI NO.	16833	16834
AL	10.0000	10.0000
AS	.0100	0
B	.0030	.0020
BA	.1000	.1000
BE	.0003	.0002
CA	1.5000	4.0000
CD	.0010	.0010
CR	.0010	.0020
CU	.0020	.0030
FE	2.0000	1.5000
GA	.0001	.0001
K	1.5000	1.0000
LI	.0003	.0010
MG	.3000	.3000
MN	.0300	.0400
MO	.0100	.0200
NA	.5000	.4000
NB	.0005	.0010
P	.0500	.0300
PB	.0060	.0070
SI	10.0000	10.0000
SR	.0700	.0300
TI	.3000	.2000
V	.0050	.0700
Y	.0020	.0010
YB	.0001	.0001
ZN	.0100	.0200
ZR	.0080	.0100

ELEMENTS NOT FOUND:
AG AU BI CD CE CS DY ER EU GD GE HF HG HO IN IR LA LU ND NI OS PD PR PT RB RE RH RU SB SC SE SM SN TA TB TE TH TL TM U W

X.0000 DESIGNATES A CONCENTRATION GREATER THAN X PERCENT.

I FTND 0060 STOP
EOJ

REQUISITION NUMBER 400011
DATE 03/26/76

SEMIQUANTITATIVE EMISSION SPECTROGRAPHIC ANALYSIS
ELEMENT COMPARISON IN PERCENT

LPI NO.	17064
AG	.0001
AL	10.0000
BA	.0200
BE	.0003
CA	4.0000
CO	.0030
CR	.0010
CU	.0700
FE	4.0000
GA	.0001
HG	.0200
K	1.0000
MG	.4000
MN	.0600
MO	.0400
NA	.4000
NB	.0020
NI	.0030
P	.0300
PB	.0300
SC	.0010
SI	10.9999
SN	.0040
SR	.0500
TI	.5000
V	.0300
W	.0200
Y	.0050
YB	.0001
ZN	.0200
ZR	.0400

ELEMENTS BELOW DETECTION LIMIT
AS AU BI CD CE CS GE LA LI PT RB SB TA TE TH TL U

X.9999 DESIGNATES A CONCENTRATION GREATER THAN X PERCENT.

#0# EQUALS ELEMENT BELOW DETECTION LIMIT

I FTNO 0060 STOP
EOJ

APPENDIX BI

EVALUATION OF TEST BLOCK MATERIAL

EVALUATION OF TEST BLOCK MATERIAL

Procedure

Thin sections were made of samples 16833 and 16834. Each thin section was examined under a petrographic microscope and a complete simiquantitative model analysis was performed. The results of these analyses are presented in Table 1, Appendix BI. Heavy minerals were separated from the samples using bromoform. The heavy minerals were then examined under a microscope and visual estimates of mineral percentages were made. The results of this work are presented in Table 2, Appendix BI. No uranium minerals could be found or identified in either sample.

Summary of Findings

Samples 16833 and 16834 were found to consist of variable amounts of quartz, chert, chalcedony, plagioclase, K-feldspar, volcanic rock fragments, plutonic rock fragments, sedimentary rock fragments, hornblende, biotite, muscovite, chlorite/penninite, calcite, pyroxene, epidote, and opaques (Table 1, Appendix BI). The heavy mineral suites of both samples were found to consist of magnetite, hematite, ilmenite, biotite, muscovite, epidote, zircon, pyroxene, garnet, hornblende, chlorite, and sphene (Table 2, Appendix BI).

Table 1 Appendix BI

MINERALOGY OF SAMPLES

Mineral/Component	Percent in Sample Number 16833	16834
Quartz	26	18
Chert	6	4
Chalcedony	tr	tr
Plagioclase	9	6
K feldspar	2	2
Volcanic RF	25	45
Plutonic RF	14	11
Sedimentary RF	14	11
Hornblende	2	tr
Biotite	tr	tr
Muscovite	tr	tr
Chlorite/penninite	tr	--
Calcite	tr	tr
Pyroxene	tr	tr
Epidote	tr	tr
Opaques	tr	1

Table 2 Appendix BI

HEAVY MINERAL ANALYSIS

Mineral	Percent in Sample Number 16833 *	16834 *
Magnetite	50	48
Hematite	13	18
Ilmenite	9	10
Biotite	5	6
Muscovite	4	2
Epidote	10	10
Zircon	tr	tr
Pyroxene	1	tr
Garnet	1	tr
Hornblende	5	5
Chlorite	1	tr
Sphene	tr	tr

*The heavy mineral fraction constitutes 6.43 percent of sample 16833 and 6.10 percent of sample 16834.

Sample Mineralogy

Samples 16833 and 16834 were both found to consist of variable amounts of quartz, chert, chalcedony, plagioclase, K feldspar, volcanic rock fragments, plutonic rock fragments, sedimentary rock fragments, hornblende, biotite, muscovite, chlorite/penninite, calcite, pyroxene, epidote, and opaques (Table 1, Appendix BI). Due to their similar mineral compositions, mineral/component descriptions will be conducted simultaneously.

Quartz occurs as subangular to subrounded grains of variable size. Although single grain (common plutonic) quartz is the dominant variety, volcanic and polycrystalline varieties of quartz were also observed. Chert occurs as subangular to subrounded grains displaying the typical microcrystalline texture. Veins of secondary quartz, and inclusions of opaques and carbonate were frequently observed within chert grains. Chalcedony occurs as subangular to subrounded grains displaying the typical feathery texture. Plagioclase occurs as subangular to subrounded grains displaying minor to moderate alteration to kaolinite/sericite. Occasional zonation suggests that some were derived from volcanic rocks. Inclusions of epidote were frequently observed within plagioclase grains. K feldspar (microcline and microcline perthite) occurs as subangular to subrounded grains displaying only minor alteration to kaolinite/sericite. Volcanic rock fragments occur as subangular to subrounded clasts of variable mineralogy and rock type. Diabases, basalts, andesites, and tuffs are but a few of the rock types identified. Essentially the volcanic rock fragments consist of a groundmass which can be either alphanitic or phaneritic with phenocrysts of zoned plagioclase (often lath-shaped), biotite, pyroxene, hornblende (often rimmed by opaques) and opaques (Figure 1, Appendix BI). Epidote was observed as a replacement mineral in some of the clasts. Silicification of the groundmass and replacement of plagioclase by calcite were frequently observed. The plutonic rock fragment suite consists of subangular to subrounded fragments of what probably are granites and monzonites. Quartz, plagioclase, K feldspar, muscovite, and biotite are the principal constituents of the plutonic rock fragments (Figure 2, Appendix BI). A few gneiss fragments composed of quartz, plagioclase, and hornblende were observed in each sample. The sedimentary rock fragment suite consists of subrounded, somewhat elongated siltstone and mudstone clasts. They essentially consist of mixtures and combinations of quartz, plagioclase, K feldspar, chert, opaques, biotite, muscovite, and zircon cemented or supported by either calcite, silica, limonite, or clay (Figure 3, Appendix BI). Hornblende, biotite, muscovite, chlorite/penninite, calcite, pyroxene, epidote, and opaques occur in trace amounts as disseminated grains throughout the samples (Figure 4, Appendix BI).

a.

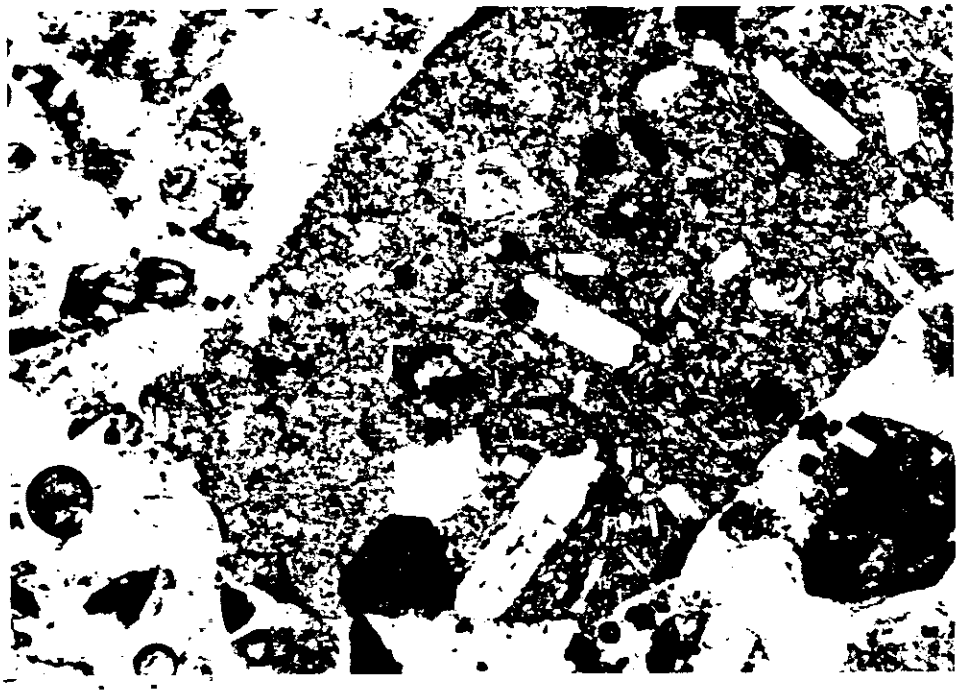

b.

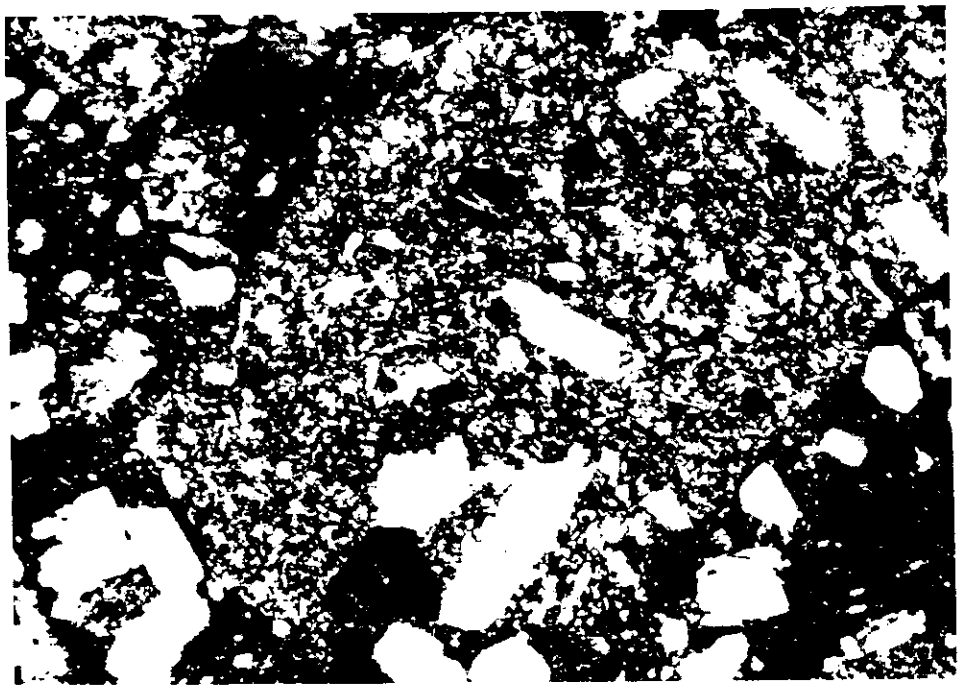

Figure 1

Appendix BI. Photomicrographs of a volcanic rock fragment consisting of an aphanitic, somewhat altered groundmass with phenocrysts or grains of zoned plagioclase, hornblende rimmed by opaques, pyroxene, and opaques. Sample 16834, a) parallel nicols, 40X, b) crossed nicols, 40X.

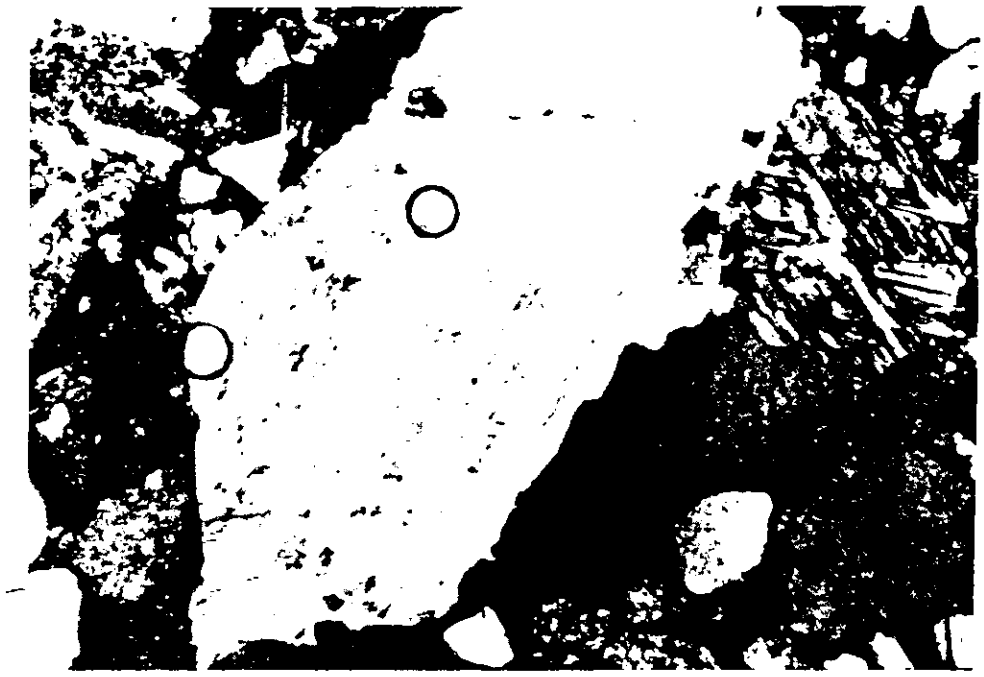

Figure 2
Appendix BI. Photomicrograph of a portion of a plutonic rock fragment composed of quartz and microline. Sample 16834, crossed nicols, 40X.

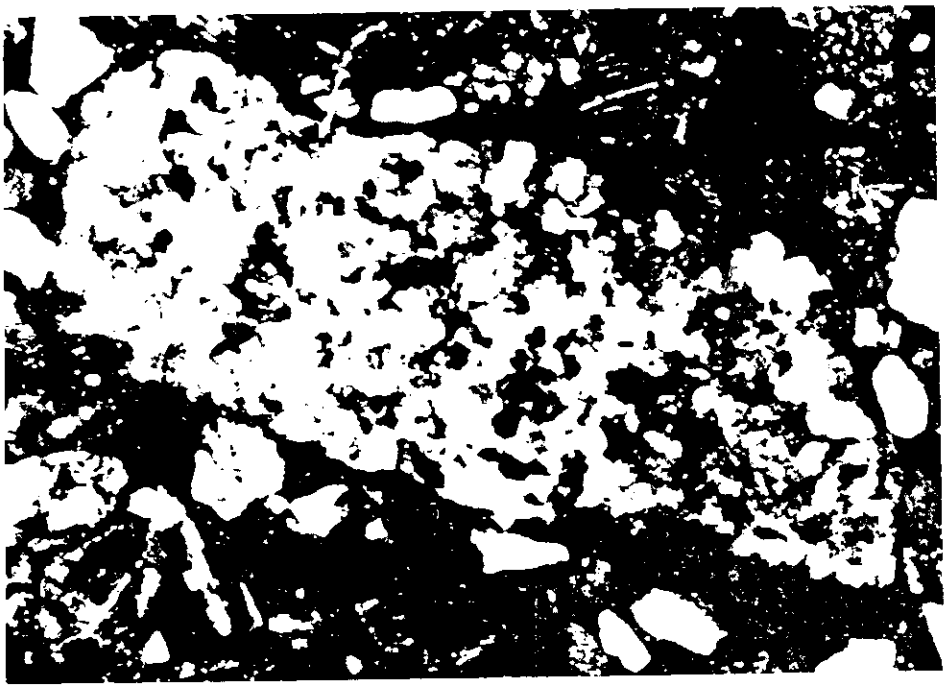

Figure 3
Appendix BI. Photomicrographs of subrounded elongate siltstone clast consisting of quartz, plagioclase, chert, and Kfeldspar grains cemented by calcite. Sample 16834, crossed nicols, 40X.

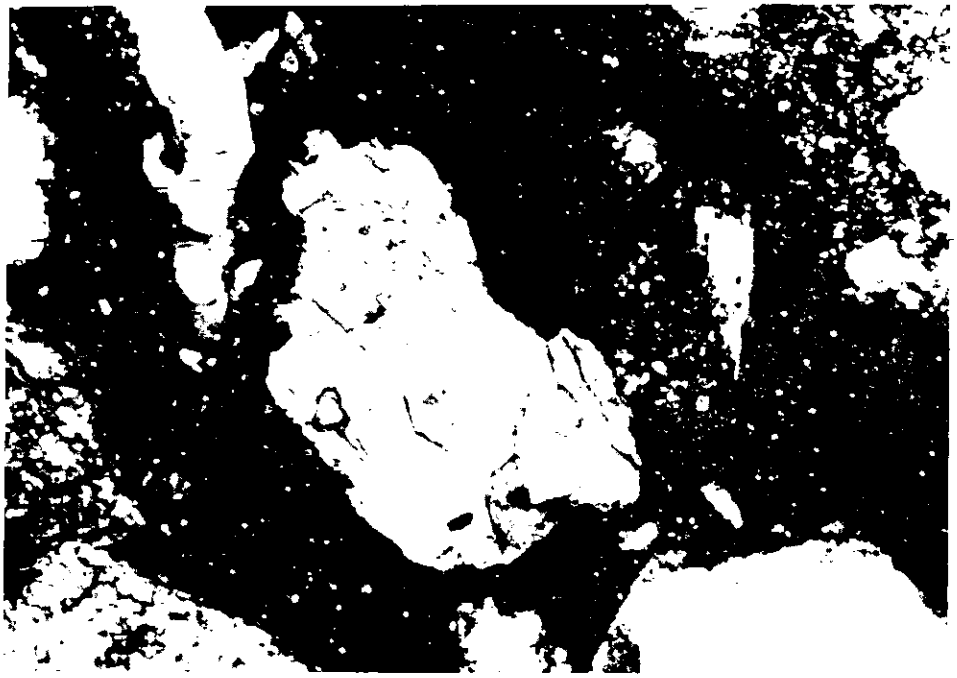

Figure 4
Appendix BI. Photomicrographs of a hornblende grain containing inclusions of quartz and biotite. Sample 16834, crossed nicols, 160X.

EVALUATION OF BLOCK MATERIAL

Procedure

Thin sections were made of representative portions of samples 16604, 16605, and 16606. Thin sections were examined under a petrographic microscope. Point counts were performed on each sample so that the percentages of the various minerals/components could be determined. The results of these point counts are presented in Table 3, Appendix BI. The heavy minerals of each sample were extracted using bromoform and were then examined using a binocular microscope. The results of these examinations are presented in Table 4, Appendix BI. No primary or secondary uranium minerals could be found or identified in any of the samples.

Summary of Findings

All three samples were found to consist of quartz, K-feldspar, plagioclase, volcanic rock fragments, plutonic rock fragments, sedimentary rock fragments, chert, hornblende, pyroxene, muscovite, biotite, chlorite, gypsum and opaques (Table 3, Appendix BI). The heavy mineral suites were found to consist of magnetite, hematite, ilmenite, pyrite/marcasite, hornblende, olivine/pyroxene, biotite, muscovite, chlorite, zircon, epidote, garnet, and sphene (Table 4, Appendix BI).

Table 3 Appendix BI

MINERALOGY OF SAMPLES

Mineral/Component	Percent in Sample Number 16604	16605	16606
Quartz	28	33	27
K-feldspar	10	5	1
Plagioclase	5	5	3
Volcanic RF	32	27	33
Plutonic RF	7	9	11
Sedimentary RF	11	12	21
Chert	4	7	2
Hornblende	tr	tr	tr
Pyroxene	tr	tr	tr
Muscovite	tr	tr	tr
Biotite	tr	tr	tr
Chlorite	tr	tr	tr
Gypsum	tr	tr	tr
Opaques	1	tr	tr

Table 4 Appendix BI

HEAVY MINERAL ANALYSIS

Mineral	Percent in Sample Number 16604*	16605*	16606*
Magnetite	46	46	38
Hematite	14	11	15
Ilmenite	8	6	5
Pyrite/Marcasite	tr	-	-
Hornblende	13	16	16
Olivine/Pyroxene	4	5	6
Biotite	5	5	6
Muscovite	3	3	4
Chlorite	1	1	1
Zircon	2	2	2
Epidote	2	3	5
Garnet	1	1	1
Sphene	tr	tr	tr

* The heavy mineral fraction constitutes 3.80 percent of sample 16604, 3.46 percent of sample 16605, and 2.59 percent of sample 16606.

Sample Mineralogy Description

All three samples were found to consist of quartz, K feldspar, plagioclase, volcanic rock fragments, plutonic rock fragments, sedimentary rock fragments, chert, hornblende, pyroxene, muscovite, biotite, chlorite, gypsum, and opaques (Table 3, Appendix BI). Due to the similarity of the samples, their mineralogies will be discussed simultaneously.

Quartz occurs as single grains (common plutonic), as polycrystalline grains, as vein quartz, and as quartz of volcanic origin. The K feldspar content consists of microcline, orthoclase, and perthite which show minor to moderate alteration to kaolinite/sericite (Figure 5, Appendix BI). Plagioclase occurs as occasionally zoned grains which also show minor to moderate alteration to kaolinite/sericite (Figure 6, Appendix BI). The volcanic rock fragment suite consists predominantly of basalt fragments (Figure 7, Appendix BI), with lesser amounts of tuffs, diorite porphyries, diabases, and others which are too altered to make positive identification. The porphyries commonly consist of a silicified groundmass with phenocrysts of quartz, plagioclase, biotite, hornblende, pyroxene, and opaques (Figure 8, Appendix BI). The plutonic rock fragment consists primarily of granitic rocks composed of quartz, K feldspar, plagioclase, muscovite, biotite, epidote, chlorite, and opaques. The sedimentary rock fragment suite consists of siltstones, sandstones, mudstones, clay clasts, calcareous sandstones and siltstones, and limestones (Figures 9, 10, Appendix BI). Chert occurs as grains displaying the typical microcrystalline texture (Figure 11, Appendix BI). Hornblende, pyroxene, muscovite, biotite, chlorite, gypsum, and opaques occur in trace amounts within the samples (Figure 12, Appendix BI).

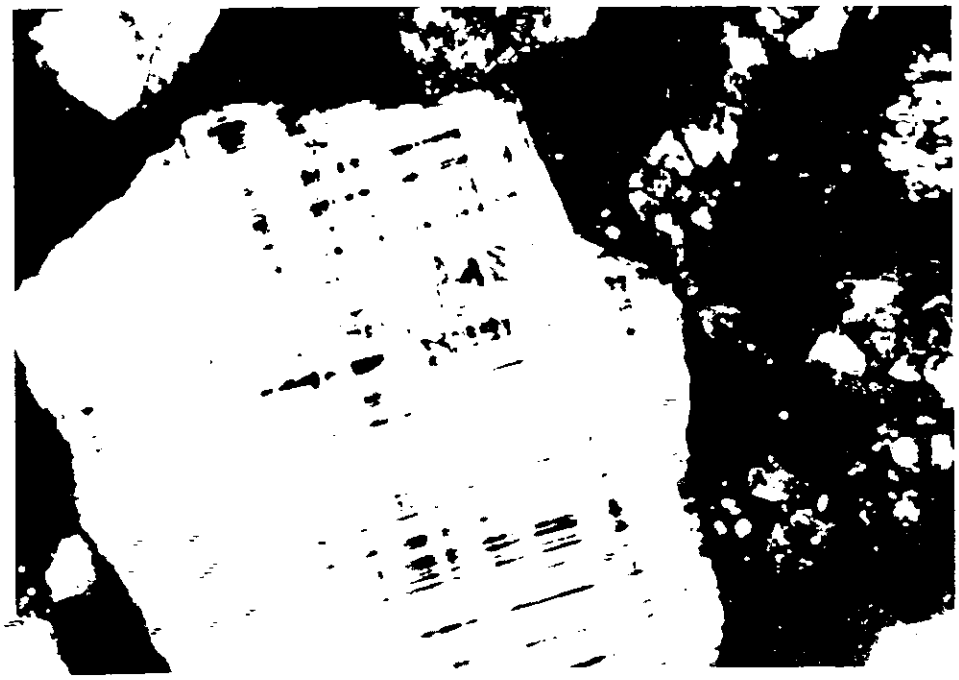

Figure 5
Appendix BI. Photomicrographs of a microcline grain displaying minor alteration to kaolinite/sericite. Sample 16605, crossed nicols, 160X.

Figure 6
Appendix BI. Photomicrographs of a plagioclase grain displaying minor alteration to kaolinite/sericite. Sample 16604, crossed nicols, 160X.

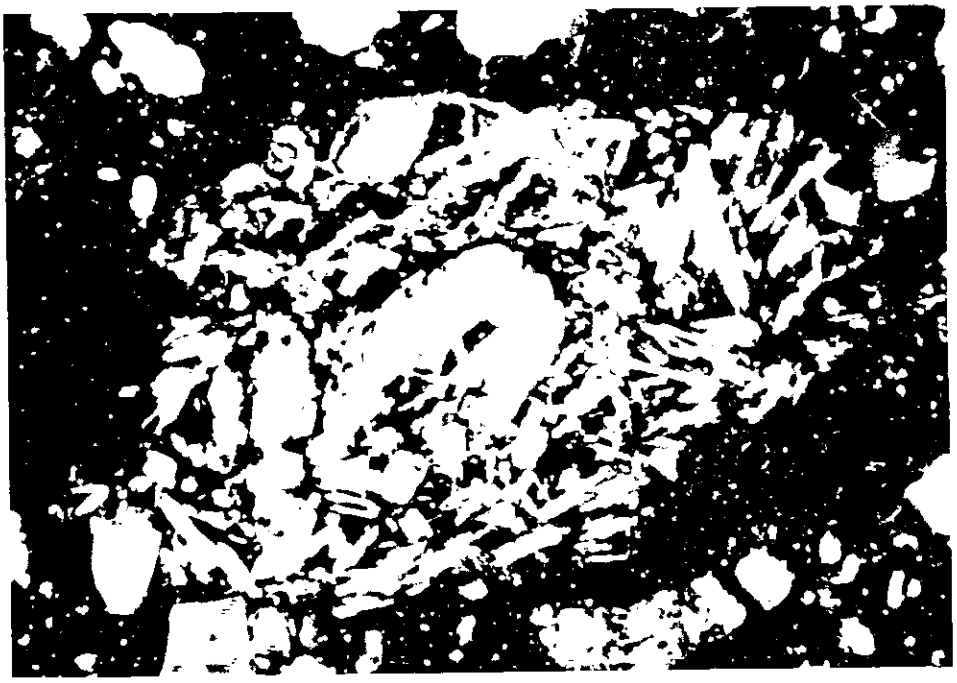

Figure 7
Appendix BI. Photomicrographs of a basalt clast composed of pyroxene and laths of plagioclase. Sample 16606, crossed nicols, 40X.

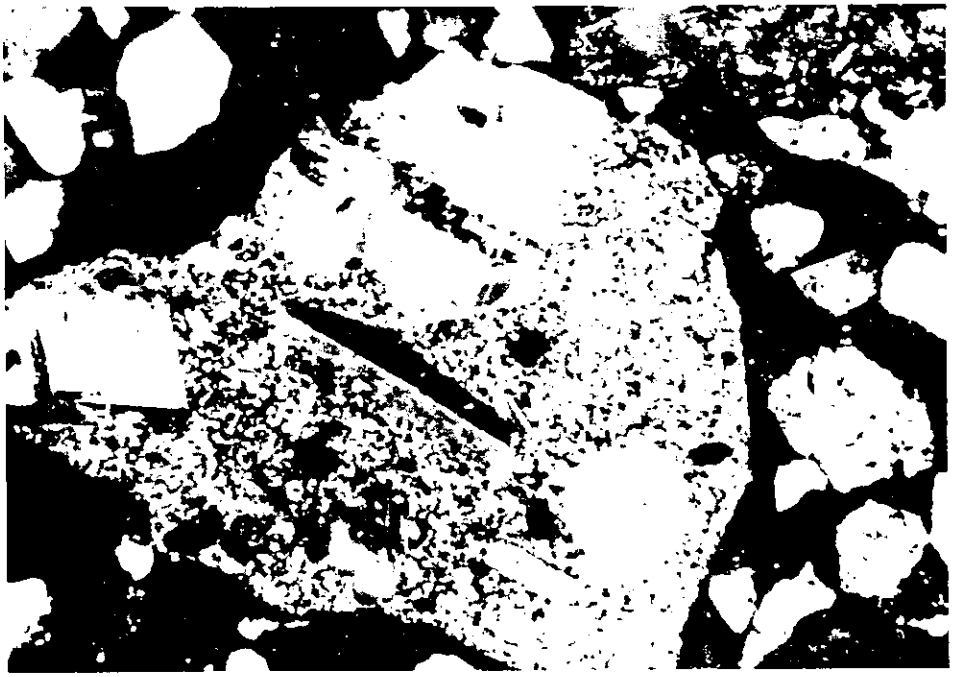

Figure 8
Appendix BI. Photomicrographs of a porphyritic volcanic rock fragment composed of silicified groundmass with phenocrysts of plagioclase, quartz, hornblende, and opaques. Sample 16604, crossed nicols, 40X.

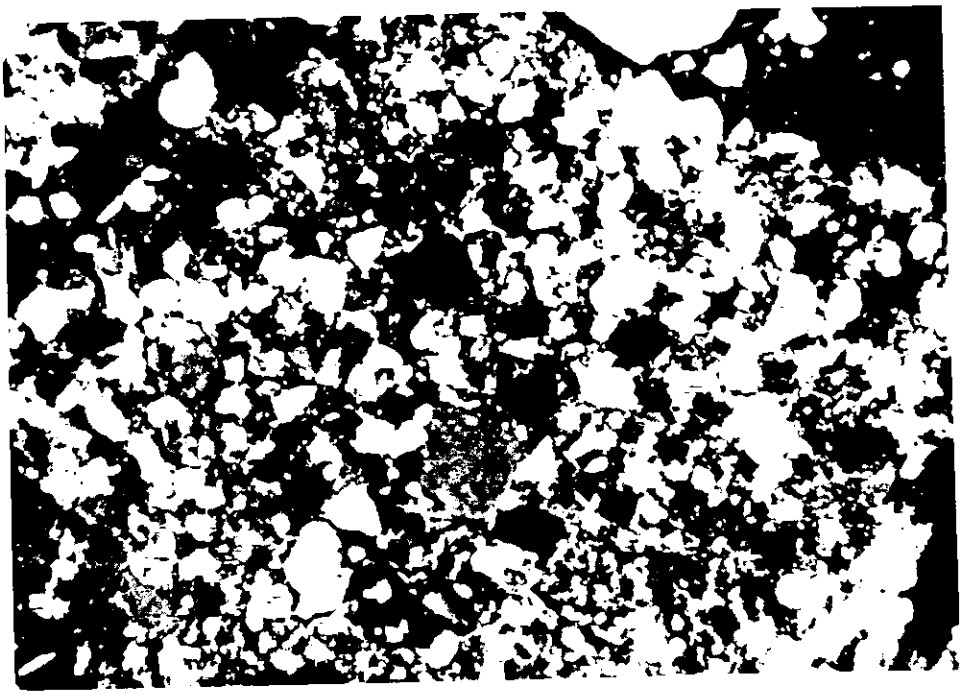

Figure 9
Appendix BI. Photomicrographs of a siltstone fragment composed primarily of quartz. Sample 16606, crossed nicols, 40X.

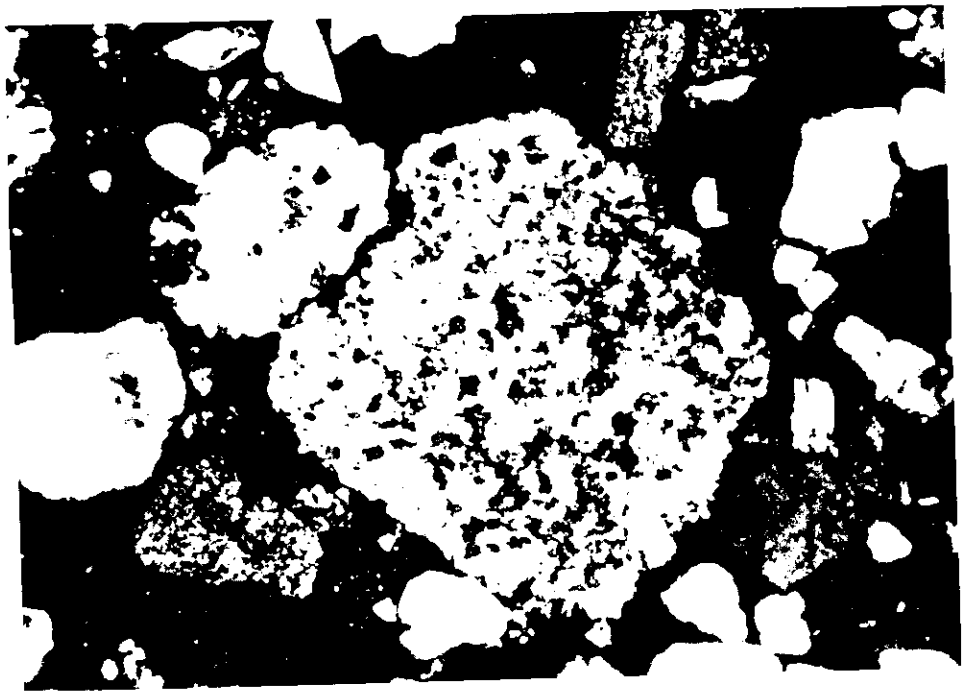

Figure 10
Appendix BI. Photomicrographs of a limestone clast (center) and a calcareous siltstone fragment. Sample 16604, crossed nicols, 50X.

Figure 11
Appendix BI. Photomicrographs of a chert fragment displaying the typical microcrystalline texture. Sample 16604, crossed nicols, 160X.

Figure 12
Appendix BI. Photomicrographs of a biotite flake in sample 16605, crossed nicols, 160X.

EVALUATION OF BLOCK MATERIAL

Procedure

Thin sections were prepared from representative portions of sample 17064. Thin sections were examined and point-counted so that the percentages of various minerals and other constituents could be determined. The results of this analysis are presented in Table 5, Appendix BI.

The heavy minerals were separated using bromoform and then examined using a binocular microscope. The results of this analysis are presented in Table 6, Appendix BI.

Contact print tests were employed to determine the presence of uranium. No uranium minerals could be found or identified in this sample.

Summary of Findings

Sample 17064 was found to consist of quartz, K feldspar, plagioclase, plutonic rock fragments, volcanic rock fragments, sedimentary rock fragments, chert, chalcedony, chlorite, biotite, muscovite/sericite, hornblende, pyroxene, epidote, garnet, and opaques (Table 5, Appendix BI). The heavy minerals found in the sample were magnetite, hornblende, hematite, muscovite, biotite, ilmenite, epidote, pyroxene, garnet, chlorite, zircon, and sphene (Table 6, Appendix BI).

Table 5 Appendix BI

MINERALOGY OF SAMPLE

Mineral/Component	Percent in Sample 17064
Quartz	24
K feldspar	6
Plagioclase	4
Plutonic RF	10
Volcanic RF	29
Sedimentary RF	16
Chert	9
Chalcedony	tr
Chlorite	tr
Biotite	tr
Muscovite/sericite	tr
Hornblende	tr
Pyroxene	tr
Epidote	tr
Opaques	1

Table 6 Appendix BI

HEAVY MINERAL ANALYSIS

Mineral	Percent in Sample 17064*
Magnetite	43
Hornblende	16
Hematite	15
Muscovite	7
Biotite	5
Ilmenite	4
Epidote	4
Pyroxene	3
Garnet	2
Chlorite	tr
Zircon	tr
Sphene	tr

* The heavy mineral fraction constitutes 8.75 percent of sample 17064, by weight.

Sample Mineralogy

Sample 17064 was found to consist of quartz, K feldspar, plagioclase, plutonic rock fragments, volcanic rock fragments, sedimentary rock fragments, chert, chalcedony, chlorite, biotite, muscovite/sericite, hornblende, pyroxene, epidote, and opaques (Table 5, Appendix BI).

Quartz commonly occurs as single, subrounded to subangular grains (both plutonic and volcanic in origin) and occasionally as polycrystalline grains, and as vein quartz. K feldspar consists dominantly of microcline and less frequently of perthite and orthoclase. Grains are commonly subrounded to subangular and occasionally show minor alteration to kaolinite/sericite. Plagioclase grains are subrounded to subangular and show minor to moderate alteration to kaolinite/sericite (Figure 13, Appendix BI). Occasional zonation of grains is observed with inclusions of apatite common. The plutonic rock fragments are predominantly granitic and composed of quartz, K feldspar, plagioclase, biotite, muscovite, epidote, garnet, sphene, hornblende, chlorite, and opaques (Figure 14, Appendix BI). They are commonly rounded to subrounded with their feldspars showing minor to moderate alteration to kaolinite/sericite. The volcanic rock fragment suite consists dominantly of andesite porphyries (Figure 15, Appendix BI) with lesser amounts of diorite porphories, diorites, rhyolites, tuffs, and many others which are extensively altered and unidentifiable. The porphyries commonly have an aphanitic, silicified groundmass with phenocrysts of quartz, plagioclase, K feldspar, biotite, hornblende, pyroxene, epidote, opaques, and chlorite/penninite (Figure 16, Appendix BI). These rock fragments are rounded to subrounded and moderately altered. The sedimentary rock fragment suite consists of rounded siltstones, mudstones, sandstones, calcareous sandstones, clay clasts, and limestones (Figure 17, Appendix BI). Chert was observed displaying the typical microcrystalline texture and was occasionally ferruginous or spherulitic. Opaques occur as irregular grains within the sample. Chalcedony, chlorite, biotite, muscovite/sericite, hornblende, pyroxene, epidote, and garnet (Figure 18, Appendix BI)occur in trace amounts in the sample.

Figure 13
Appendix BI. Photomicrographs of a plagioclase grain displaying moderate alteration to kaolinite/sericite. Sample 17064, crossed nicols, 160X.

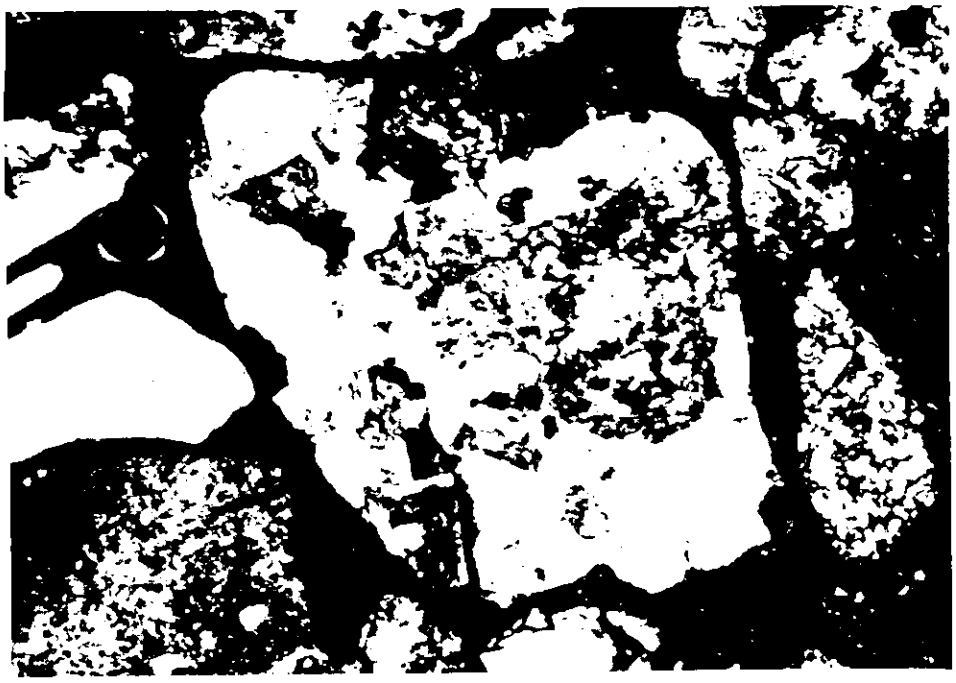

Figure 14
Appendix BI. Photomicrographs of a plutonic rock fragment composed of quartz, plagioclase, K-feldspar, epidote, sphene, biotite, and chlorite. Sample 17064, crossed nicols, 40X.

Figure 15
Appendix BI. Photomicrographs of an andesite porphyry clast composed of zoned plagioclase laths, quartz, biotite, sericite, and chlorite. Sample 17064, crossed nicols, 40X.

a.

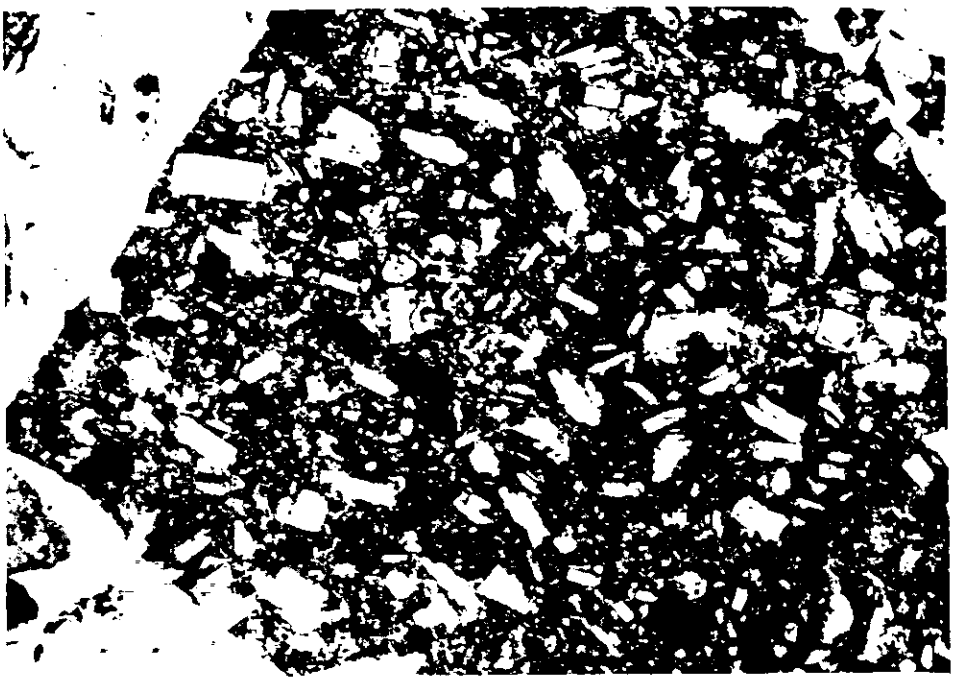

b.

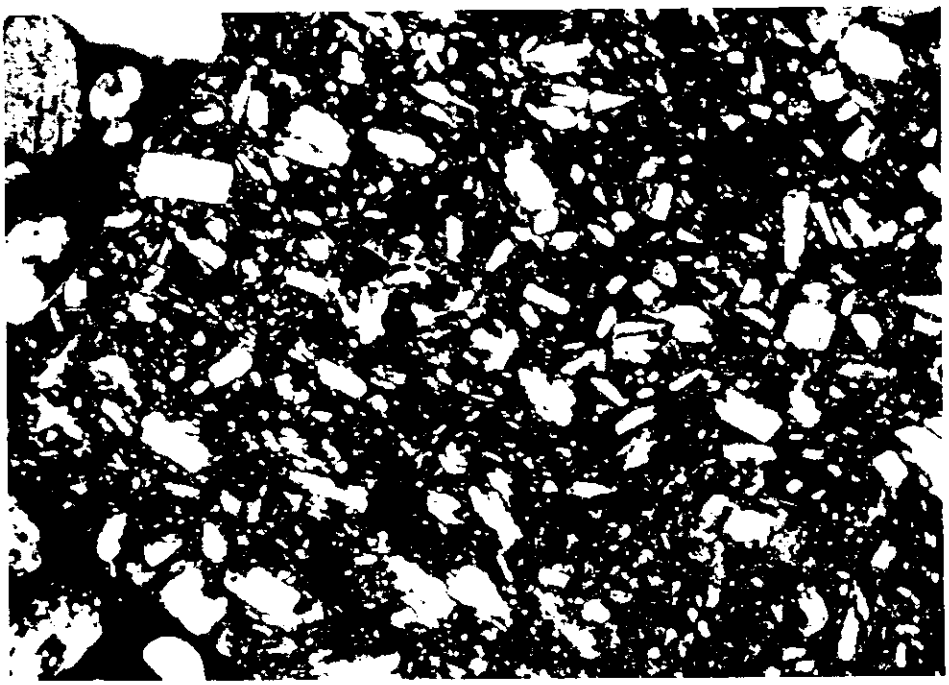

Figure 16

Appendix BI. Photomicrographs of a volcanic rock fragment with phenocrysts of plagioclase, quartz, hornblende, pyroxene, chlorite, and opaques. Sample 17064, a) parallel nicols, 40X, b) crossed nicols, 40X.

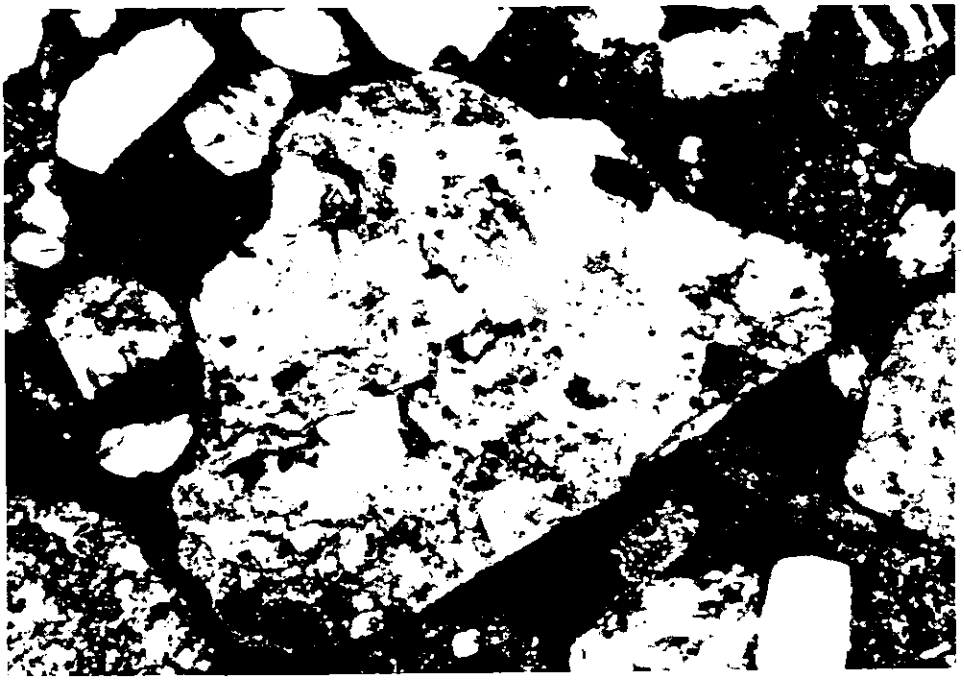

Figure 17
Appendix BI. Photomicrographs of a limestone clast which is sparitic in composition. Sample 17064, crossed nicols, 40X.

a.

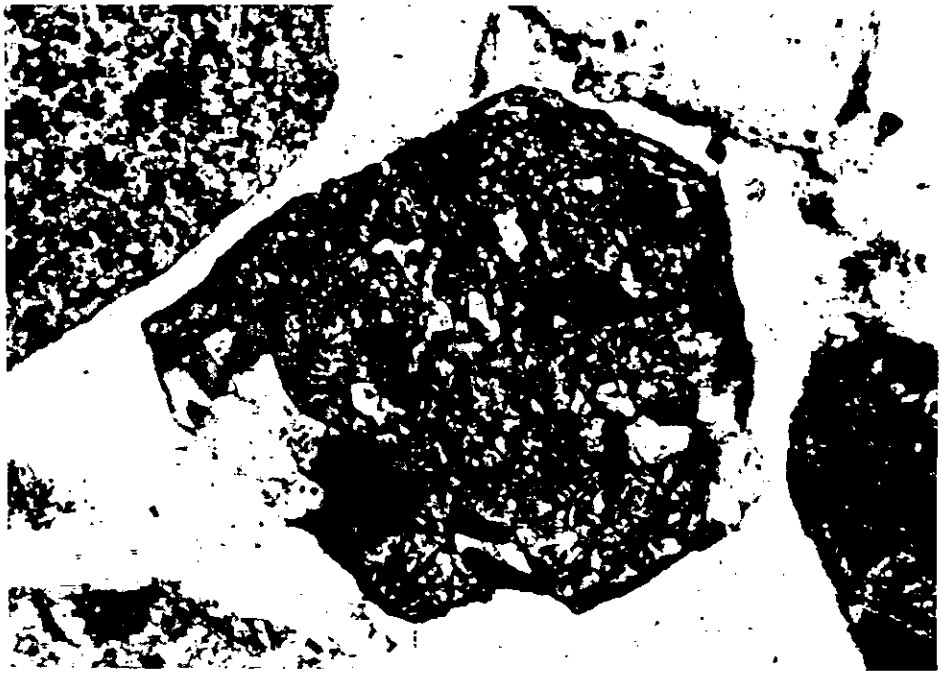

b.

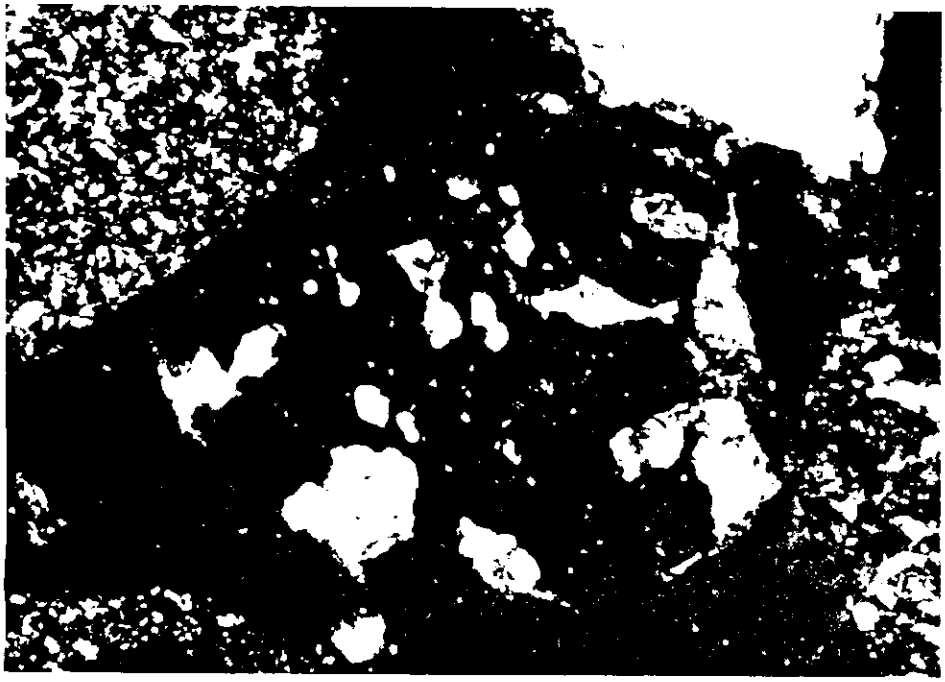

Figure 18

Appendix BI. Photomicrographs of a garnet grain with inclusions of quartz and biotite. Sample 17064, a) parallel nicols, 40X, b) crossed nicols, 40X.

PART II. GROSS GAMMA CALIBRATION BLOCK; GRADE ASSIGNMENT

ABSTRACT

"Best" grades were assigned to a series of blocks constructed by BFEC-DOE/GJO for the purpose of calibrating hand-held gross gamma counters. The grade assignment procedure followed is based on a standard least squares technique for limiting sampling errors. The assigned grades are:

Block Number	Assigned Dry Weight Grade	
	Percent eU_3O_8	ppm eU
GJ 50	0.0094 ± 0.0003	80 ± 3
GJ 200	0.0303 ± 0.0006	257 ± 5
LASL 500	0.0720 ± 0.0011	611 ± 9
GJ 1000	0.144 ± 0.002	1220 ± 20
GJ 3000	0.334 ± 0.004	2830 ± 40
CW 200	0.0313 ± 0.0006	265 ± 5
CW 1000	0.149 ± 0.002	1260 ± 20
GWT 200	0.0316 ± 0.0006	268 ± 5
GWT 1000	0.147 ± 0.002	1250 ± 20
GNM 200	0.032. ± 0.0006	272 ± 5
GNM 1000	0.145 ± 0.002	1230 ± 20

Prefix Definitions

GJ These blocks will remain at Grand Junction, Colorado.

LASL This block was sent to Los Alamos Scientific Laboratory.

CW These blocks were sent to Casper, Wyoming.

GNM These blocks were sent to Grants, New Mexico.

GWT These blocks were sent to George West, Texas.

GROSS GAMMA-RAY CALIBRATION BLOCKS; GRADE ASSIGNMENT

Introduction

For the purposes of this report, sampling error is defined as the error in any measurement resulting from the assumption that measurements made on a subset of a population generates the same result as measurements that represent the total population. In general, the larger the subset or the more homogeneous the population, the smaller the sampling error. In the case of the gross gamma calibration blocks constructed by BFEC, some sampling error is an expected result because of practical and physical constraints inherent in the construction. That is, a relatively small number of samples were withdrawn for analysis, and inhomogeneities are always present in concrete due to separation of coarse and fine materials in the pouring process, poor mixing, etc. In this case, the blocks were intended to be used as gross gamma calibration standards, so a technique to determine and limit sampling error was required. A discussion of the procedure used to assign gross gamma grades to these calibration blocks is necessary.

During construction, only three samples were taken from each block and prepared for gross gamma assay by the BFEC Geochemical Analysis Department. Each block was assigned an interim grade equal to the average of the gross gamma results from these samples. These interim grades were not used as the final grade assignment because they did not account for sampling errors that might have occurred. In making the final grade assignment, differential face scanners* were used to record gross gamma count rates from each block.

* Differential face scanners are normal scintillation counters that are fitted with removable lead shields between their detectors and the material being counted. Count rates are recorded with and without the shield. For a more complete discussion, see Appendix A II.

In the concentration design range of the various blocks and under the conditions of the experiment, the count rates are a linear function of "effective" block concentration. Here "effective" block concentration is used to account for effects such as slight inhomogeneities in the blocks, possible small scale radiometric disequilibrium, and differences in moisture content between blocks. Multiple readings were taken and averaged for each block to reduce statistical error. The points (count rate versus interim block concentration) were plotted and fitted by a straight line using the least-squares technique. To the extent that the average count rate observed for each block reflects the effective concentration of ore at the location of the detector, these count rates establish the effective concentration of the block. The effective concentrations were the new concentrations determined using the average count rate and the parameters determined for the least-squares curve. Four sets of data were recorded, each using a different differential face scanner, to further reduce sampling errors and to check for instrumental errors. The effective concentration of the blocks obtained for the four data sets was averaged using a weighting procedure based on the statistical uncertainties of each set of results. These weighted averages were used as the assigned gross gamma concentrations of the blocks.

Low-Concentration Check of Gross Gamma Analyses

The gross gamma analyses performed by the BFEC Geochemical Analysis Department on the calibration block samples were to be used as the basis for the grade assignment. These analyses were checked by independently running a set of standards that were in the concentration range of the

block samples. This check was particularly important, because the calibration standard for the gross gamma instrument ranged from 4 to 150 times the concentration of the block samples. This procedure demonstrated that operational deficiencies in the gross gamma technique occurred when low concentration material was analyzed. Specifically, the counting times were too short. Corrections for the short counting times were carried out for the low concentration block samples and the standards. The results of the gross gamma analysis of these low concentration standard materials are listed in Table II-I. Note that reasonably good agreement exists between the known standard concentrations and the gross gamma results.

Sample Density Considerations

There is experimental and theoretical evidence suggesting that a correction is necessary in all types of laboratory gamma analysis of bulk samples when the densities of the sample and the calibration standard are different. Conceptually, an experiment can be imagined in which a can filled with an unknown sample is counted; the can is opened and the same volume is filled with twice as much sample. Again, the can is counted. Although there is twice as much sample in the can, the count rate is not twice as great, because some fraction of gamma rays emitted by the additional sample material is absorbed. In gross gamma analysis, the unknown concentration is determined by the expression

$$\text{Unknown Concentration} = (\text{K factor}) \frac{(\text{Observed Count Rate})}{(\text{Weight of Sample})}.$$

In the experiment described above, the weight would have doubled but the count rate would not. Therefore, two different concentrations would be reported, when, in fact, only the density (sample mass/can volume) had

changed. Errors resulting from density effects can be expected to be largest when conditions favor absorption of the gamma-rays (i.e., thick cans and/or low energy gamma-rays). Fortunately, relatively thin cans are used in the gross gamma analysis and low energies are filtered out instrumentally. When these conditions exist, the density corrections should not be large. Unfortunately, at the present, we have not determined the exact techniques for making these density corrections. Accordingly, density information is included with all radiometric data presented in this report, although no corrections currently are made.

Table II-I. Check of the Low Concentration Calibration of the Gross Gamma Instrument

NBL Reported Standard Concentration %U (chemical)(a)	Standard Concentration $\%eU_3O_8$ (b)	Gross Gamma Results $\%eU_3O_8$ (c)	Ratio of Densities of Standard Materials (d)
0.0101 ± .0002	0.0122 ± .0002	0.0124 ± .0.0009	0.98
0.051 ± .001	0.0618 ± .0010	0.0611 ± 0.0014	0.90
0.104 ± .002	0.126 ± .002	0.123 ± 0.005	0.90

(a) Uncertainties are at the 95 percent confidence level (2σ).

(b) In addition to converting from $U \rightarrow U_3O_8$ using the factor of 1.179, an additional factor of 1.027 was used to correct the NBL grades for known disequilibrium.

(c) Results are the average of four gross gamma determinations with their standard deviation.

(d) This is the ratio of net can weights for the gross gamma calibration standard and the material being analyzed. There is reason to believe that analysis results will be in error when there is a significant density difference between the calibration standard and the sample material being analyzed.

Block Moisture Considerations

Grade assignments for the calibration blocks are made in terms of dry weight concentration because this method most nearly represents the information sought in field measurements. However, the pads are not dry (see Table II-II for block moisture contents). The moisture content has two practical ramifications which affect field procedures and influence grade assignment.

When material is encountered in the field which has significantly different formation moistures than those found in the calibration blocks, a correction factor should be used in calculating uranium concentrations. This correction factor accounts for the difference in gamma-ray attenuation due to moisture. In the absence of good information concerning either formation moistures encountered in the field or the appropriate moisture correction factor, the uncertainty limits of reported concentrations may be significant.

In grade assignment, differential count rates are plotted against the dry weight uranium concentration as determined by gross gamma-ray analysis. Assuming that no sampling errors or statistical fluctuations in analysis have occurred, the data should fall on a straight line. It is also assumed that there are no physical differences between blocks. The variations in the moisture content from block to block cause a scattering of the data points about the best-fit curve. However, new grades (called effective grades) can be assigned to the blocks using the radiometric data, recorded on the blocks, to normalize to the average moisture content of the blocks. This is a valid approach and a desirable one because the effective grades are the grades the blocks would appear to have in gamma counting experiments. Normalization to average moisture content was carried out for these gross gamma-ray blocks.

The procedure used is identical to that used to correct for sampling errors. In fact, when the procedure is used to correct for one effect, the other effect is also corrected.

Table II-II. Comparison of Block Moisture Content

Block Identification	%Loss on Drying (a)	Relative Neutron Probe Response (b)	%Moisture, Free & Hydrated Water (c)
GJ 50	2.68	544	7.03
GJ 200	2.80	550	7.78
LASL 500	2.93	540	8.56
GJ 1000	3.61	510	8.55
GJ 3000	2.81	532	3.50
CW 200	2.68	545	8.17
CW 1000	3.57	501	9.69
GNM 200	2.43	546	7.94
GNM 1000	3.56	511	8.32
GWT 200	2.45	554	8.22
GWT 1000	3.58	502	8.41
Average	3.01	—	7.79

(a) Core samples were heated to 110°C until constant weight was obtained. Each number is usually the average of four samples.

(b) These responses were obtained with the subsurface neutron tool lying on top of each block. Even though the tool could not be calibrated for this geometry, the degree of consistency of the measurements could be taken to indicate the relative variations in the moisture content of the blocks.

(c) At the time of the pouring, one sample was collected from each block and allowed to air dry. From the known amount of water added in preparation of the concrete and the weight loss on drying, the percent free and hydrated water was determined. For example, when the concrete for block GJ-50 was prepared, 15.0 percent water by weight was added to the mix. A sample was taken at the time of pouring and was allowed to air dry. The sample weight decreased 8.0 percent on drying. Thus, the percent moisture and hydrated water was 7.0 percent.

Prefix Definitions

GJ - These blocks will remain at Grand Junction, Colorado.

LASL - This block was sent to Los Alamos Scientific Laboratory.

CW - These blocks were sent to Casper, Wyoming.

GNM - These blocks were sent to Grants, New Mexico.

GWT - These blocks were sent to George West, Texas.

Laboratory Gross Gamma Results

Three samples withdrawn as each block was poured (near the beginning, near the middle, near the end) were assayed using a laboratory gross gamma-ray technique. These concrete samples were allowed to set up; then a portion of each sample was crushed, dried, and sealed inside gross gamma analysis cans.* Conventional laboratory gross-gamma analyses were performed on these samples. After canning, the samples were aged for several hours and then counted with the gross gamma system. The samples were counted a second time, approximately 24 hours later. Based on the rate of increase in the observed activity, resulting from the regeneration of radon lost during sample preparation, the equilibrium activity was calculated for each sample; this activity was used to establish the equivalent uranium concentration. Again, based on the increase in activity between the two counting intervals, the activity at the time of canning was calculated; the difference between this activity and the activity at equilibrium corresponds to the amount of radon lost during sample preparation. The ratio of the amount of radon lost to the amount of radon at equilibrium (indicated in each case by the apparent uranium concentrations) is defined as the relative emanation coefficient. The equivalent uranium concentrations and the relative emanation coefficients from the gross gamma analysis are reported in Table II-III.**

---

* See Part I of this report entitled "Gross Gamma-Ray Calibration Blocks; Construction," for a complete discussion of the construction, sampling, chemical analysis, and petrographic analysis of these blocks.

** For a more complete discussion of the gross gamma technique, see "Gamma-Only Assaying for Disequilibrium Corrections" by J. H. Scott and P. H. Dodd, April 1960. U.S. Atomic Energy Comm. RME-135.

Table II-III. Results of the Geochemical Laboratory's Gross Gamma Assay of the Gross Gamma Calibration Block Samples

	Block Number and Sample Location	Sample Number	Net Sample Weight (grams) (a)	Gross Gamma Grade (eU_3O_8)	Relative Emanation Coefficient
GJ 50 (b,c)	bottom	17406	23.4	0.007	
	middle	07	22.6	0.008	(b)
	top	08	24.0	0.008	
	average		23.3	0.0077	
GJ 200	bottom	17409	19.9	0.038	0.34
	middle	10	21.2	0.030	0.15
	top	11	21.9	0.038	0.30
	average		21.0	0.0353	0.26
LASL500	bottom	17412	21.3	0.083	0.16
	middle	13	19.7	0.078	0.22
	top	14	20.3	0.067	0.20
	average		20.4	0.0760	0.19
GJ1000	bottom	17415	20.1	0.146	0.20
	middle	16	19.8	0.144	0.18
	top	17	19.8	0.146	0.18
	average		19.9	0.1453	0.19
GJ3000	bottom	17418	19.5	0.326	0.13
	middle	19	21.0	0.334	0.20
	top	20	20.0	0.330	0.14
	average		20.1	0.3300	0.16
GWT200	bottom	17421	19.8	0.037	0.34
	middle	22	21.2	0.032	0.21
	top	23	21.0	0.028	0.04
	average		20.6	0.0323	0.20
GWT1000	bottom	17424	19.9	0.136	0.15
	middle	25	20.6	0.143	0.15
	top	26	19.7	0.152	0.18
	average		20.1	0.1436	0.16
GNM200	bottom	17427	20.0	0.029	(d)
	middle	28	21.4	0.030	0.26
	top	29	20.4	0.029	0.13
	average		20.6	0.0293	0.20
GNM1000	bottom	17430	20.3	0.150	0.19
	middle	31	19.4	0.145	0.17
	top	32	19.9	0.146	0.17
	average		19.9	0.1470	0.18

Table II-III (cont'd)

Block Number and Sample Location		Sample Number	Net Sample Weight (grams) (a)	Gross Ga a Grade ($\mu g/m^3$ 8)	Relative Emanation Coefficient
CW200	bottom	17433	19.6	0.033	0.32
	middle	34	19.6	0.033	0.20
	top	35	19.6	0.035	0.23
	average		19.6	0.0337	0.25
CW1000	bottom	17436	19.8	0.152	0.16
	middle	37	20.4	0.160	0.22
	top	38	20.3	0.147	0.20
	average		20.2	0.1530	0.19

(a) The weight of the calibration standard used in this analysis was 272 grams.

(b) The original samples from this block were contaminated in the sampling plant and had to be reprepared from remaining core material.

(c) Extended data collection times were used for these samples to improve the statistical precision of the data.

(d) No emanation coefficient was calculated because several later count rates were lower than the first.

Prefix Definitions

GJ These blocks will remain at Grand Junction, Colorado.

LASL This block was sent to Los Alamos Scientific Laboratory.

CW These blocks were sent to Casper, Wyoming.

GNM These blocks were sent to Grants, New Mexico.

GWT These blocks were sent to George West, Texas.

Gross Gamma Face Scanner Data

After the blocks were poured and allowed to cure for several weeks, a series of differential face scanners* were used to collect data used in defining a final assignment for the blocks. The counting equipment used consisted of a Disa 400, a Disa 410 A (Exploranium), a PS 872 with a prototype scintillation probe (Mount Sopris) and a 2 inch x 2 inch crystal assembly supported by the electronics package of the BFEC-DOE/GJO surface KUT unit. These systems approximate the state-of-the-art in digital scintillometers, and each was fitted with a differential face scanner attachment. Initially, it was hoped that a series of analog scintillometers, like the SC 131 (Mount Sopris), could be used. However, experimentation with these instruments showed that they did not offer sufficient readout accuracy to be used in grade assignment.**

Four sets of data were recorded using each of the four digital scintillometers on each of the 11 blocks. Count rates recorded with and without the shield were dead time corrected and the differential count rates were (Δcps) established. Table II-IV lists the average Δcps for the four sets of gross gamma-ray data obtained with each counter used on each block. The statistical weighting factors used in making the final grade assignments, which are weighted averages of the results using each of the four counters, are reported in Table II-IV. These weighting factors were determined by the statistical uncertainty of the results obtained using each of the four counters; they are the reciprocals of the percent uncertainty for the GJ 50 block, normalized to one (in the worst case). The uncertainty is equal to

* See Appendix AII for an introductory discussion of differential face scanners and the differential face scanner technique.

** See Appendix DII for a discussion of the problems encountered using the SC 131 scintillometers, a report of K factors determined for these instruments, and an estimate of accuracy which can be expected when applying instruments with differential face scanner attachments.

Table II-IV. Gross Gamma Face Scanner Data

Block Number U		Geochemical Gross Gamma Grade Percent eU_3O_8	Face Scanner Δcps (b)			
			PS 872	BFEC 1718	Disa 400	Disa 410A
GJ	50	0.0077	89	69	64	38
GJ	200	0.0353	310	224	222	101
LPSL	500	0.0760	707	562	516	224
GJ	1000	0.1453	1410	1116	1040	489
GJ	3000	0.3300	3190	2570	2595	1166
CW	200	0.0337	313	240	224	96
CW	1000	0.1530	1438	1126	1125	498
GWT	200	0.0323	314	241	221	108
GWT	1000	0.1436	1428	1123	1084	470
GNM	200	0.0293	314	247	232	103
GNM	1000	0.1470	1417	1125	1079	447
Weighting Factor (c)			4	7	2	1

a) These are the average of the laboratory results for the three samples taken from each block.

b) These are the average of the results from four sets of data on each block.

c) The weighting factors were determined by the statistical uncertainty of the results from each instrument; they are the reciprocals of the uncertainties for the GJ50 block, normalized to one in the worst case.

Prefix Definitions

GJ These blocks will remain at Grand Junction, Colorado.

LASL This block was sent to Los Alamos Scientific Laboratory.

CW These blocks were sent to Casper, Wyoming.

GWT These blocks were sent to George West, Texas.

GNM These blocks were sent to Grants, New Mexico.

the square root of the sum of the count rates with and without the differential shield. The percent uncertainty reflects the crystal size, the gross gamma threshold, the proximity of the detector to the block, and the effectiveness of the shield.

Gross Gamma Grade Assignments

The first step in using the data collected in the laboratory and on the blocks is to correct for sampling errors; the approach used is to plot the average differential count rates as a function of the average block grade determined from the samples withdrawn at the time the blocks were poured. This plot (for each scintillometer) is shown in Figure II-I with the linear least squares fit of the data. The best known point in the curve is, of course, the origin (0,0). The detector response curve was forced through the origin by entering three data points corresponding to (0,0), for each data point, when performing the least squares fit (weighting the origin point). This weighting has the effect of limiting the influence of random errors, in the data near the origin, that might otherwise adversely affect the data. Table II-V lists the slope and intercept for the linear fits to each data set.

The next step in assigning corrected grades to the blocks is to determine the equivalent uranium grade for each block using the differential count rates and the linear curve parameters. This approach incorporates the laboratory gross gamma results of all 33 samples (3 samples from each of the 11 blocks) into the determination of the grade of each block. The results of this approach are listed in Table II-VI along with the statistical weighting factors previously determined for each counting system. The final step required to assign block grades is to take the weighted average of the four results for each block. These weighted averages are the assigned calibration grades for the blocks, corrected for sampling errors and small moisture variations between blocks. These values are the assigned dry weight uranium grades for gross gamma calibration blocks listed in Table II-VII. The one-sigma uncertainties in Table II-VII reflect a combination of calculated error analysis, the observed standard deviation of the results,

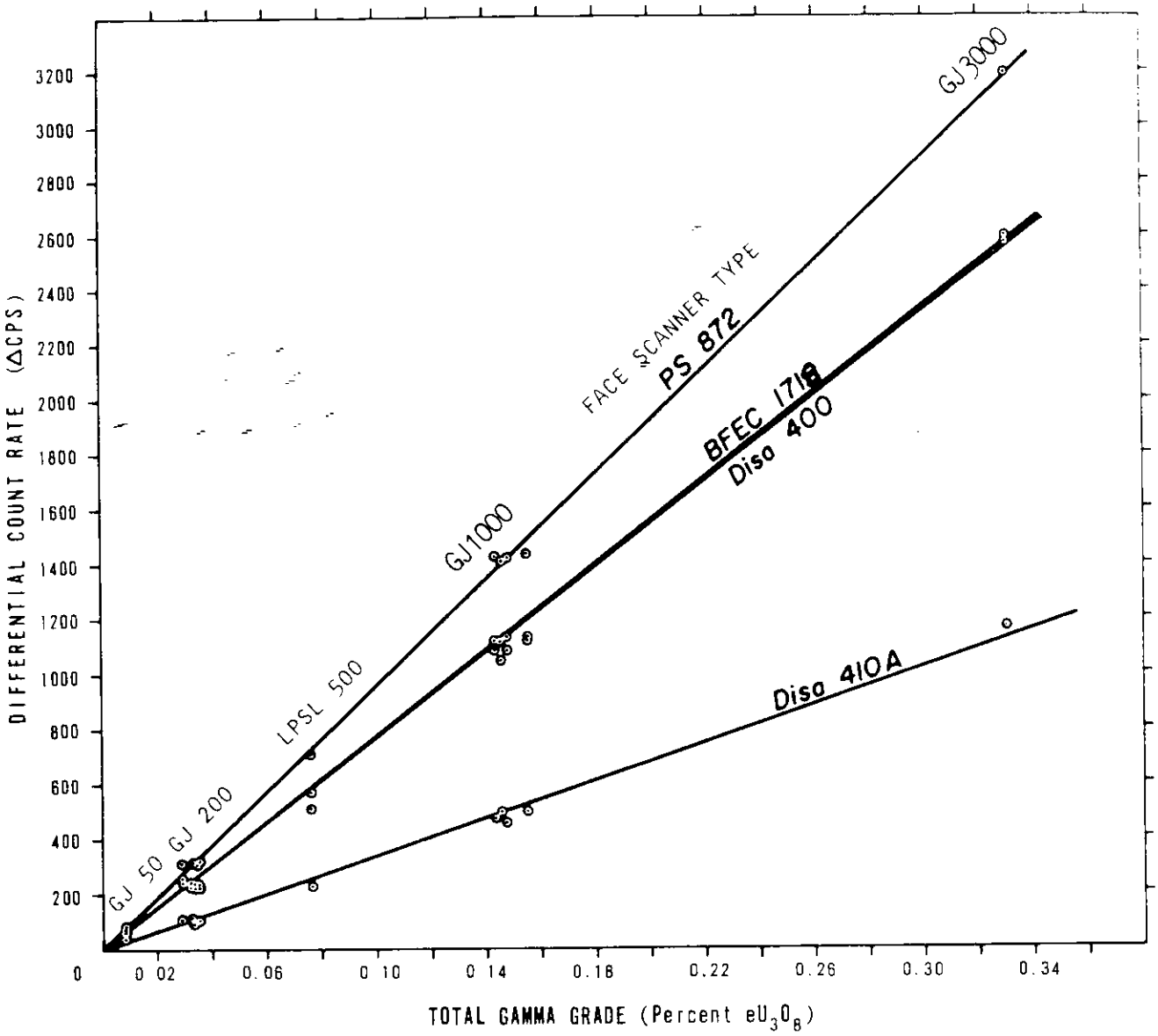

Figure II-I. Differential Count Rate versus Total Gamma Grade for the eleven uranium calibration blocks using four different differential face scanner counting systems.

Table II-V. K Factors for Instruments Used in Calibration

Instrument	Slope in Figure 1 (Δcps/%eU_3O_8)	Intercept in Figure 1 Δcps (a)	K Factor	
			%eU_3O_8/Δcps	ppm U/Δcps
Mount Sopris hand Face Scanner PS 872	9.65×10^{3}	-2.18	1.036×10^{-4}	8.79×10^{-5}
BFEC (1718) 2 x 2 Probe	7.71×10^{3}	-2.04	1.30×10^{-4}	1.10×10^{-4}
Exploranium Disa 400	7.69×10^{3}	-2.44	1.30×10^{-4}	1.10×10^{-4}
Exploranium Disa 410A	3.40×10^{3}	-4.88	2.94×10^{-4}	2.49×10^{-4}

(a) In an attempt to force the detector response curve through the origin, three data points corresponding to the origin (0,0) were entered for each data point in Table II-IV.

Table II-VI. Calculated Block Grades Using the K Factors Reported in Table II-V

Block Number (ppm U)		Calculated Grades Percent eU_3O_8 (a)				Weighted Average
		PS 872	BFEC 1718	Disa 400	Disa 410A	
GJ	50	0.0094	0.0092	0.0090	0.0119	0.0094
GJ	200	0.0323	0.0293	0.0294	0.0305	0.0303
LASL	500	0.0734	0.0732	0.0677	0.0667	0.0720
GJ	1000	0.1462	0.1451	0.1358	0.1447	0.1440
GJ	3000	0.3306	0.3338	0.3380	0.3441	0.3340
CW	200	0.0326	0.0314	0.0298	0.0290	0.0313
CW	1000	0.1491	0.1464	0.1469	0.1474	0.1470
GWT	200	0.0327	0.0315	0.0294	0.0325	0.0316
GWT	1000	0.1481	0.1460	0.1546	0.1391	0.1470
GNM	200	0.0327	0.0323	0.0310	0.0310	0.0321
GNM	1000	0.1470	0.1463	0.1409	0.1323	0.14502
Weighting Factor (b)		4	7	2	1	

a) Calculated using slopes and intercepts listed in Table II-V and the average Δcps listed in Table II-IV.

b) The weighting factors were determined by the statistical uncertainty of the results from each instrument; they are the reciprocals of the uncertainties for the GJ 50 block, normalized to one for the worst case.

Prefix Definitions

GJ These blocks will remain at Grand Junction, Colorado.

LASL This block was sent to Los Alamos Scientific Laboratory.

CW These blocks were sent to Casper, Wyoming.

GWT These blocks were sent to George West, Texas.

GNM These blocks were sent to Grants, New Mexico.

Table II-VII. Concentration Assignments for the Gross Gamma Calibration Blocks

Block Number U	Assigned Dry Weight Grade (a)	
	Percent eU_3O_8	ppm eU
GJ 50	0.0094 ± 0.0003	80 ± 3
GJ 200	0.0303 ± 0.0006	257 ± 5
LASL 500	0.0720 ± 0.0011	611 ± 9
GJ 1000	0.144 ± 0.002	1220 ± 20
GJ 3000	0.334 ± 0.004	2830 ± 40
CW 200	0.0313 ± 0.0006	268 ± 5
CW 1000	0.149 ± 0.002	1260 ± 20
GWT 200	0.0316 ± 0.0006	268 ± 5
GWT 1000	0.147 ± 0.002	1250 ± 20
GNM 200	0.0321 ± 0.0006	272 ± 5
GNM 1000	0.145 ± 0.002	1230 ± 20

a) These reported uncertainties reflect a combination of calculated error analysis, the observed standard deviation of the results, and estimates of absolute calibration errors of standard materials. They are at the 67 percent confidence level. These errors do not take into account the error resulting from the influence of sample density.

Prefix Definitions

GJ These blocks will remain at Grand Junction, Colorado.

LASL This block was sent to Los Alamos Scientific Laboratory.

CW These blocks were sent to Casper, Wyoming.

GWT These blocks were sent to George West, Texas.

GNM These blocks were sent to Grants, New Mexico.

and estimates of absolute calibration errors of standard materials; however, they do not take into account the error resulting from the influence of sample density.

There are important considerations that should be considered. First, systematic errors in either the laboratory data or the block data are not corrected by this procedure; the result would be a difference in slope for the curves in Figure II-I. Fortunately, sampling errors, moisture variations, and statistical counting errors are usually random errors. Furthermore, when any one data point reflects a very large error, this error will be reduced for the point in question but will cause increased error in other points. However, this situation can easily be identified by inspection of the fit of the data to the straight lines. For example, the series of points for the GJ 50 block were relatively far removed from the least squares curve. Examination of the KUT laboratory results showed that contamination of the sample material had occurred during sample preparation. A second set of samples prepared from this block did not exhibit this difficulty.

Conclusions

Examination of the data presented in Figure II-1 suggests that it was necessary to perform this type of error reduction technique in assigning grades to the gross gamma-ray calibration blocks. For example, consider the set of four data points for the LASL 500 block having a grade of about 0.08 percent eU_3O_8; each of the data points fall below the least-squares curve. This result strongly suggests that the grade determined by laboratory analysis contained a significant sampling error. Furthermore, consider the spread of values reported for four blocks poured from the same batch of cement having grades of approximately 0.03 and 0.15 percent eU_3O_8. In either case, the spread of values found for these blocks was about four times greater in the laboratory analysis of withdrawn samples than it was in the analysis of each of the blocks as a unit. Finally, the contamination that occurred in preparing the original set of samples from block GJ 50 would not have been detected, if this sampling error reduction procedure had not been used.

APPENDIX AII

Introduction to the Differential Face Scanner Technique

The principle difficulty in using conventional (non-differential face scanner) equipment for quantitative field measurements is the 4¶ solid angle sensitivity of the gamma detector. Unless the calibration and all counting is performed in the same geometry, errors result. Suppose a scintillometer is calibrated using a circular block of material 1 foot in diameter with the detector at a fixed distance above the block; further, suppose a geologist in the field--with this same counter--happens to find two circular blocks of the same material. For illustration, the first block is 1 foot in diameter and the second is 2 feet in diameter. Although the two blocks are of the same material and have the same radiometric concentrations, the count rates of the two blocks will be different; and different concentrations will be measured. The different count rates should be expected, because the detector is not sensitive to gamma-rays from just the 1 foot circular area; it also detects some fraction of the gamma-rays coming from the additional material of the larger block. In this case, it is the concentration determined using the 1 foot block that is correct, because it is the same geometry as that used in calibration. Clearly, the extra material in the larger block influences the counting rate, and any other material in the general area of the detector will affect the counting rate. Often it is impractical to subtract background count rates, because sometimes the background cannot be differentiated from the signal. In the counting experiment described above, the count rate from the first foot of the larger block can be considered to be signal, and the count rate from the remaining portion of the block can be considered to be background. Thus, to the extent that

counting geometry differs between calibration and counting, or that backgrounds from other material in the vicinity of the detector cannot be adequately corrected, errors must be expected.

Modifying the above experiment, suppose the detector is fitted with a removable shield just large enough and thick enough to absorb all the gamma-rays coming from a circular area 1 foot in diameter. In the field, the geologist takes two readings on each sample, one without the shield and one with the shield; hence, the accuracy of the assays is significantly improved. The first reading, without the shield, corresponds to the count rate from all material in the area including that material which is being assayed. The second reading, with the shield in place, corresponds to the count rate from all materials in the area except the material being assayed. Therefore, the difference between the first and second reading is just the count rate coming from the material being assayed. When the two blocks in the above example are counted, a different count rate is observed with and without the shield for each of the blocks; however, the same differential count rate is observed for both blocks. Thus, the same concentration is assigned both blocks.

An alternative method to using a differential filter which shields the source is to shield everything but the source. Although only one measurement is taken on each sample to be assayed, this is a poor alternative because it would be necessary to carry much heavier shielding (on the order of 150 pounds) in the field. The weight difference between this total shielded method and the differential shielded technique is large, because the differential filter is inherently smaller and because it is not necessary for the differential filter to be 100 percent effective in stopping the gamma-rays from the material being assayed. If only a

fraction of gamma-rays are stopped by the filter, the fraction stopped is still proportional to the original number emitted by the source and can, therefore, be used to determine the radiometric concentration of the source.*

Reducing the weight of the shield by accepting a less effective filter, does not result in a "get something for nothing" situation. Under these circumstances, it is necessary to count for a longer time to obtain the same statistical precision. For example, the differential count rate is the difference between the unshielded count rate and the shielded count rate. That is,

$$D = U - S,$$

where D = Differential count rate,

U = Unshielded count rate, and

S = Shielded count rate.

However, the uncertainty in D is the square root of the sum of U and S, or

$$d = (U + S)^{1/2},$$

where d = uncertainty in D.** As the shield is made thinner, D becomes smaller (S becomes more nearly equal to U) and d, the uncertainty in D, increases.

Clearly, there are many field situations in which the differential counting technique is inappropriate, but when a quantitative measurement is necessary and the counting geometry is substantially different from that used in calibration, the differential counting technique should be

---

* In the argument above, explicit consideration was not given to the fact that for each gamma-ray energy a different fraction of the gamma-rays will be stopped by the differential filter. This effect is not great provided the shape of the spectrum is not radically different for the calibration source and for the field samples. Generally, this energy distribution is not a problem when bulk samples are used as calibration sources.

** For a more complete discussion of statistics of radiometric counting, see any introductory text on nuclear physics.

considered. The differential counting technique can also be applied to gamma-ray spectral methods.

APPENDIX BII

Edge Effects on the Gross Gamma Blocks

When calibrating a differential face scanner on a block, it is desirable to have the block only slightly larger than the area shadowed by the filter. This configuration yields the best statistical precision when calibrating. Using the face scanner technique, the uncertainty of any measurement is the square root of the sum of the number of counts recorded with and without the filter. This uncertainty has the smallest percentage value when the number of counts recorded with the filter is as large as possible and the number of counts recorded without the filter is as small as possible. In this case, the differential count rate will be maximized while the uncertainty is minimized. This conclusion favors small diameter blocks. Conversely, when calibrating conventional scintillometers, it is desirable to have very large blocks which approximate an infinite plane. The gross gamma calibration blocks described in Part I are 42 inches in diameter and 17-18 inches thick. Based on preliminary calculations, this block size appeared to be a reasonable compromise. To check the applicability of these blocks in calibrating conventional scintillometers, a series of measurements were made of the observed total count as a function of radial distance from the center of the block. In this experiment, a Mount Sopris model SC 131 scintillometer fitted with a differential counting filter was used. Figure 1, Appendix BII shows the total count (without filter) and the differential count data. These data show that the differential count is not influenced by the position of the instrument until it is very near the edge of the block. Then the edge of the block begins to fall within the area shadowed by the filter. The total count data, however, clearly indicate that the count rate has not yet reached a constant value (leveled off) at the center of the block. If

a constant count rate value had been obtained, the block would approximate an infinite block. Fortunately, the total count does reach a value within 5 to 10 percent of that expected for an infinite plane. This approximation to an infinite block is quite acceptable considering the large errors expected when the nondifferential technique is applied in the field (see Appendix AII for a discussion).

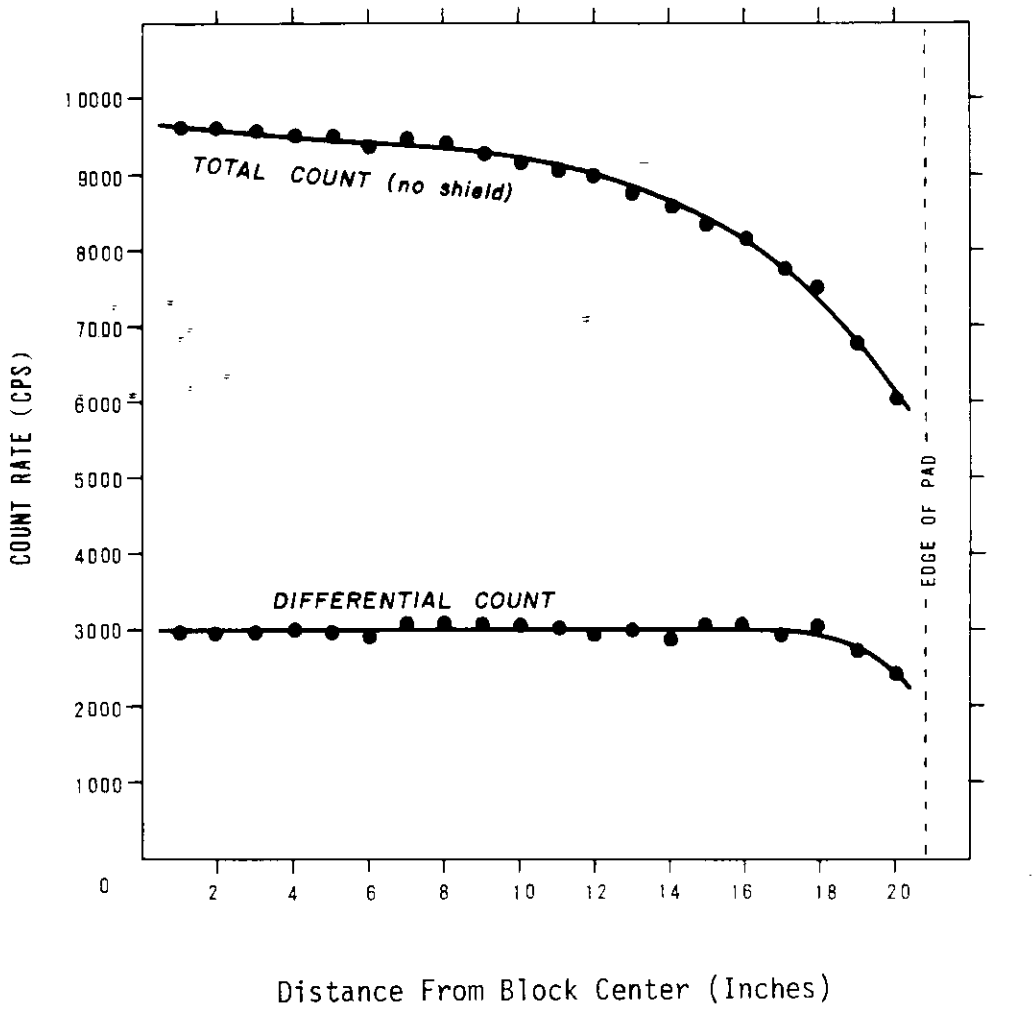

A Mount Sopris model SC-131A scintillometer fitted with a differential counting shield was used for this comparison.

Figure 1, Appendix BII. A comparison of the sensitivity of total count and differential count methods to the proximity of the edge of a 3300 ppm calibration block.

APPENDIX CII

General Radiometric Homogeneity of the Gross Gamma Blocks

Differential face scanners yield results characteristic of the material shadowed by the filter plate, whereas conventional counters yield results that are influenced by material considerably more remote from the counter. If the gross gamma blocks are used to calibrate these conventional gamma-ray counters, it is important to know that the grade assignment made for the center of the block (marked by a 1 inch black spot) is appropriate for the entire surface of the block. To confirm this conclusion, a series of readings were taken at various locations on each block using a Mount Sopris Model SC-131 scintillometer with a differential face scanner attachment. The locations of the measurement positions and the observed gamma-ray count rates are presented in Figure 1, Appendix CII and Table I in Appendix CII, respectively. These data show that the blocks have no large scale inhomogeneities that would prohibit their use in calibrating conventional gamma counting equipment.

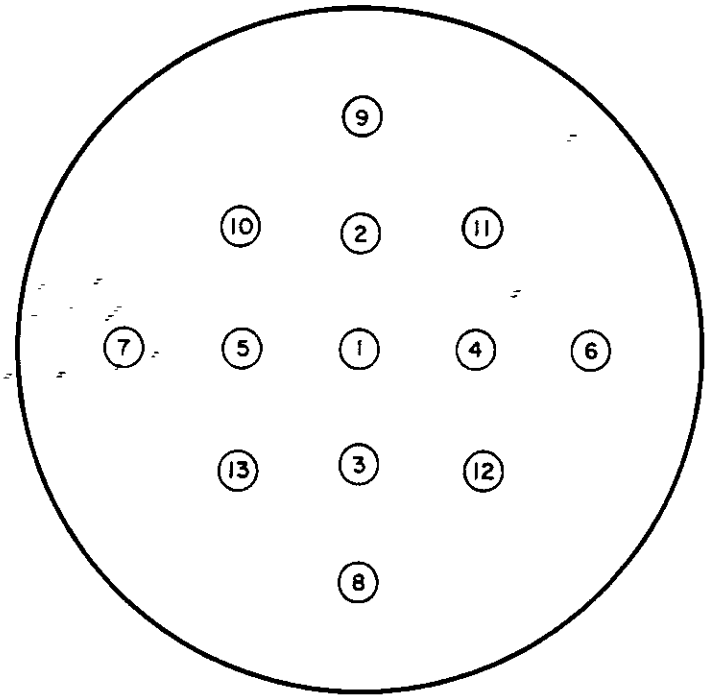

BLOCK

Figure 1, Appendix CII. Identification of the positions used to establish the general homogeneity of the gross gamma-ray calibration blocks.

Table 1, Appendix CII. Count Rates Observed on the Gross Gamma Blocks for the Purpose of Establishing General Homogeneity

Pad	Type of Reading	Count Rate (cps) at 13 Positions on Each Block (a)												
		1	2	3	4	5	6	7	8	9	10	11	12	13
GJ50	W.Shield	245	230	235	240	235	215	215	205	210	230	225	225	220
	W/O Shield	330	310	320	315	320	300	295	285	285	310	310	310	310
	ΔCPS	85	80	85	75	85	85	80	80	75	80	85	85	90
GJ200	W.Shield	740	670	660	690	680	620	620	610	600	680	690	670	670
	W/O Shield	990	960	960	970	960	880	870	850	860	940	950	930	920
	ΔCPS	250	290	300	280	280	260	250	240	260	260	260	260	250
LASL 500	W.Shield	1420	1320	1380	1320	1320	1080	1100	1080	1100	1280	1260	1280	1280
	W/O Shield	1940	1880	1900	1900	1880	1640	1680	1660	1660	1820	1820	1840	1820
	ΔCPS	520	560	520	580	560	560	580	580	560	540	560	560	540
GJ1000	W.Shield	2900	2750	2650	2800	2650	2100	2100	2000	2100	2400	2450	2400	2400
	W/O Shield	4050	3900	3650	3950	3800	3100	3150	3050	3150	3450	3500	3400	3450
	ΔCPS	1150	1150	1000	1150	1150	1000	1050	1050	1050	1050	1050	1000	1050
GJ3000	W.Shield	6600	6100	6300	6200	6100	5400	5300	5300	5400	5900	6000	6000	5900
	W/O Shield	9000	8800	8700	8700	8600	7900	7700	7700	7800	8500	8400	8500	8500
	ΔCPS	2400	2700	2400	2500	2500	2500	2400	2400	2400	2600	2400	2500	2600
CW200	W.Shield	650	610	620	600	610	540	550	540	560	580	590	580	590
	W/O Shield	940	890	920	890	900	780	800	810	810	830	830	820	830
	ΔCPS	290	270	300	290	290	240	250	270	250	250	240	240	240
CW1000	W.Shield	2900	2700	2650	2750	2600	2350	2400	2400	2350	2750	2700	2700	2750
	W/O Shield	4000	3850	3750	3900	3800	3500	3450	3450	3500	3750	3700	3750	3750
	ΔCPS	1100	1150	1100	1150	1200	1150	1050	1050	1150	1000	1000	1050	1000
GWT200	W.Shield	140	130	130	140	130	150	110	110	100	120	140	140	120
	W/O Shield	440	440	420	440	420	460	380	370	370	420	440	440	410
	ΔCPS	300	310	290	300	300	310	270	260	270	300	300	300	290
GWT1000	W.Shield	2850	2650	2650	2750	2550	2400	2350	2450	2450	2750	2750	2750	2700
	W/O Shield	4050	3800	3750	3900	3700	3550	3450	3500	3500	3800	3750	3800	3750
	ΔCPS	1200	1150	1100	1150	1150	1150	1100	1050	1050	1050	1000	1050	1050
GNM200	W.Shield	660	650	650	650	650	580	570	580	580	620	620	630	630
	W/O Shield	960	950	940	950	920	820	830	830	830	860	870	870	860
	ΔCPS	300	300	290	300	270	240	260	250	250	240	250	240	230
GNM1000	W.Shield	2900	2700	2700	2800	2700	2400	2350	2350	2350	2750	2800	2750	2750
	W/O Shield	4000	3900	3900	3900	3750	3500	3500	3450	3500	3800	3750	3750	3800
	ΔCPS	1100	1200	1200	1100	1050	1100	1150	1100	1150	1050	950	1000	1050

(a) These data were taken using a Mount Sopris scintillometer model SC-131 fitted with a differential face scanner attachment. The time constant used was 16 seconds and readings were recorded only after waiting at least 1 minute.

Prefix Definitions

GJ - These blocks will remain at Grand Junction, Colorado.
LASL - This block was sent to Los Alamos Scientific Laboratory.
CW - These blocks were sent to Casper, Wyoming.
GWT - These blocks were sent to George West, Texas.
GNM - These blocks were sent to Grants, New Mexico.

APPENDIX DII

Experimentation with a SC 131A Scintillometer

Initially, we expected to use a series of Mount Sopris scintillometers, model number SC 131A, to collect the gross gamma-ray block data. However, the instrument was first tested to determine whether serious errors would result from its use. The error which is easiest to predict is the meter reading error. The smallest division on the meter of the SC 131A corresponds to 2 percent of full scale. The meter can be read accurately to about 1/2 division and the readings, on the average, will be at about 1/2 of full scale; these conditions correspond to a 2 percent reading error.

Another source of instrument error results from non-linearity of the meter movement. Also, there is an added effect due to apparent dead time losses; this effect appears as a non-linearity in the meter movement of the SC 131A because the dead time (pulse pair resolution) is a function of the range setting of this instrument. The apparent dead time is 10 times greater on the times five (X5) range than it is on the X50 range. Thus, the same percent loss of data occurs for the same meter indication, independent of the range setting of the instrument. For example, a reading of 90 on the meter, with the instrument on the X5 range, yields the same percent dead time loss as a reading of 90 on the X50 range. Neither the effect of non-linearity in the meter movement nor the effect of dead time losses can be ignored; because they manifest themselves similarly, a single experiment was conducted to examine both effects. A scale reading of 50 was defined to correspond to an error of 0 percent. The instrument was placed in a low background shield along with multiple gamma-ray sources. By positioning

the sources at fixed locations and noting the count rates singly and in combinations, the counting non-linearity of the instrument was established. In Run 1, for example, two sources were placed in the shield such that each source, independently, produced a midscale meter reading, in this case, 50 and 48. When both sources were placed in the shield, a meter reading of 98 would be expected if it were not for non-linearity and dead time losses. The meter reading in this case was only 92, or 6 percent less than expected. The results of this experiment are presented in Table I, Appendix DII, and Figure 1, Appendix DII, and range to ±6 percent of full scale.

The last source of error considered here are the errors between the various range of the instrument. In an experiment designed to detect these errors, single sources in a fixed geometry were counted with the instrument set on different ranges. The observed meter readings were corrected for the non-linearity observed above. By definition, the range X20 was chosen to be correct. The results of this experiment are presented in Table II, Appendix DII and range to -9 percent.

Considering the uncertainty in the corrections necessary to use the SC 131's and the time necessary to identify the appropriate corrections for each instrument used, digital instruments were selected for the calibration study. However, to aid those using SC 131's in the field, K factors were determined for each of the instruments. These are presented in Table III, Appendix DII.

Table 1, Appendix DII. Scale Reading Non-Linearity of Mount Sopris Scintillometer Model Number SC-131A (GJO 10026)

Run Number	Scale Readings (-Bkg.)[a]			Scale Reading Error		
	Individual	Predicted Combined	Observed Combined	At Scale Reading	Magnitude	Relative Error
				50	≡0	≡0
1	48 50	98	92	93[b]	-6%	2[c]
2	25 26	51	50	26	+2%	2
3	18 17 17	52	50	18	+4%	3
3'	18 17	34[d]	35	36	+3%	4
3"	17 17	33[d]	34	35	+3%	4
4	24 24 25	69[d]	67	68	-3%	4
4'	24 24	48	46	25	+4%	2
5	33 33 34	97[d]	93	94	-4%	5
5'	33 33	64[d]	62	63	-3%	4
6	47 49	96	90	91	-6%	2
7	14 13	27	25[d]	15	+8%	3
7'	14 13 15	39[d]	39	40	0	4

(a) All readings were taken on the (X5) scale of the scintillometer. The experiment was performed within a low background shield which resulted in a background count rate of 5 cps or 1 unit on the (X5) scale.

(b) Background count rate of 1 unit (X5) added back in at this point.

(c) Relative errors speak only to directness of the determination. If no source was used the error was ≡0, if 2 sources were used the error was assigned a value of 2, and if 2 sources were used but each was based on a value previously

assigned an error of 2, the error in the new value was assigned $(2^2 + 2^2)^{\frac{1}{2}} = 2.8 \pm 3$. A graph of these results suggests that the absolute magnitude of the error was about $\pm$ 0.5 for one relative unit.

(d) The sum of the scale readings for individual sources was corrected using information from previous runs.

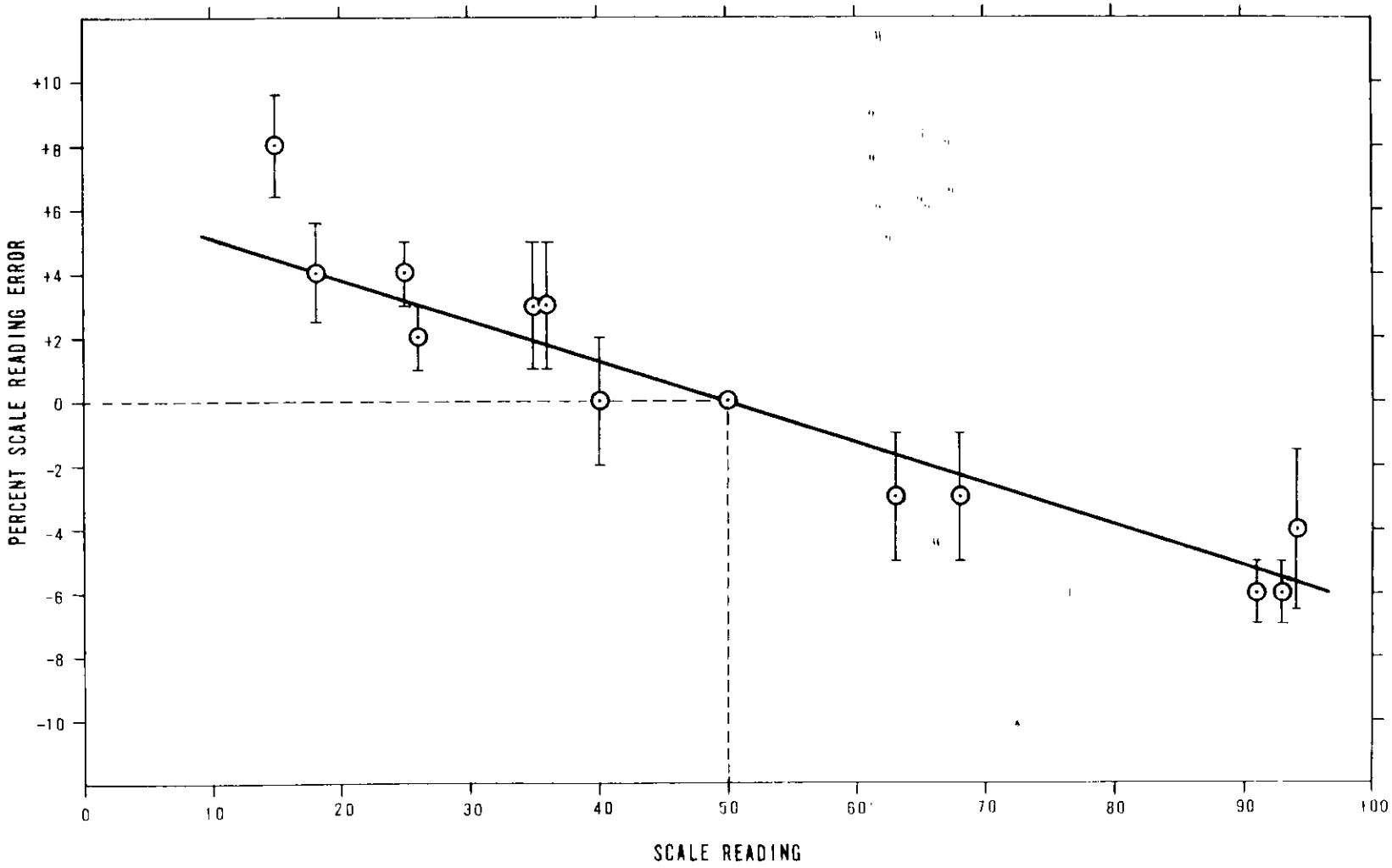

Figure 1, Appendix DII. Meter Scale Nonlinearity of Mount Sopris Model SC-131A Scintillometer GJ0-10026.

Table 2, Appendix DII. Interscale Reading Errors for Mount Sopris Scintillometer Model SC 131-A (GJO-10026)

Multiplier	Scale[a] Reading	Linearity[b] Corrected Scale Reading	Relative Interscale Error
100	19.5	1870	-9%
50	38.5	1900	-7%
20	95	2040	≡0
20	10	189	(≡0)
10	19	182	-4%
5	34	171	-2%
2	83	175	-7%
2	15	29	(-7%)
1	32	31	0%

(a) Average of two readings without changing geometry.

(b) Scale reading correction taken from Figure 1, Appendix DII "Meter Scale Non-Linearity (X5 scale) for Mount Sopris Scintillometer".

Table 3, Appendix DII. K Factors for Four Mount Sopris SC 131 Scintillometers

Scintillometer Serial Number	K Factor	
	Percent $eU_3O_8/\Delta cps$	ppm $eU/\Delta cps$
8705	1.17×10^{-4}	0.992
8706	7.95×10^{-5}	0.679
9641	1.20×10^{-4}	1.03
10026	1.27×10^{-4}	1.09

APPENDIX EII

Block ID and Serial Numbers

Serial Number	Identification of the Block	Government ID Number
1	GJ 50	GJO 10253
2	GJ 200	GJO 10254
3	LASL 500	GJO 10257
4	GJ 1000	GJO 10255
5	GJ 3000	GJO 10256
6	CW 200	GJO 10130
7	CW 1000	GJO 10131
8	GNM 200	GJO 10132
9	GNM 1000	GJO 10133
10	GWT 200	GJO 10134
11	GWT 1000	GJO 10135

The letters in the identification of the block are the location of each block.

GJ - Grand Junction
LASL - Los Alamos Scientific Laboratory
CW - Casper, Wyoming
GNM - Grants, New Mexico
GWT - George West, Texas

The numbers in the identification of the block are the nominal design grades in uranium concentration of each block.

REFERENCES

Evans, Hilton B., 1978, A Review of U.S. DOE Calibration Facilities, NEA/IAEA Workshop on Borehole Logging for Uranium, Grand Junction, Colorado, Feb. 14-16.

Kosanke, Kenneth L., 1976, Gross Gamma-Ray Calibration Blocks, Part II, Gross Gamma-Ray Calibration Blocks; Grade Assignment, GJBX-59(78).

Mathews, Mark A., 1976, Gross Gamma-Ray Calibration Blocks, Part I, Gross Gamma-Ray Calibration Blocks; Construction, GJBX-59(78).

Scott, James H. and Dodd, P. H., 1960, Gamma-Only Assaying for Disequilibrium Corrections, U.S. Atomic Energy Comm. RME-135, April.